Journal of Neurology (2019) 266:1953–1959
https://doi.org/10.1007/s00415-019-09364-3

ORIGINAL COMMUNICATION

Amyotrophy, cerebellar impairment and psychiatric disease are the main symptoms in a cohort of 14 Czech patients with the late-onset form of Tay–Sachs disease

Helena Jahnová[1] · Helena Poupětová[1] · Jitka Jirečková[1] · Hana Vlášková[1] · Eva Košťálová[1] · Radim Mazanec[3] · Alena Zumrová[4] · Petr Mečíř[2] · Zuzana Mušová[5] · Martin Magner[1]

Received: 2 December 2018 / Revised: 2 May 2019 / Accepted: 6 May 2019 / Published online: 10 May 2019

Abstract

Background Tay–Sachs disease (TSD) is an inherited neurodegenerative disorder caused by a lysosomal β-hexosaminidase A deficiency due to mutations in the *HEXA* gene. The late-onset form of disease (LOTS) is considered rare, and only a limited number of cases have been reported. The clinical course of LOTS differs substantially from classic infantile TSD.

Methods Comprehensive data from 14 Czech patients with LOTS were collated, including results of enzyme assays and genetic analyses.

Results 14 patients (9 females, 5 males) with LOTS were diagnosed between 2002 and 2018 in the Czech Republic (a calculated birth prevalence of 1 per 325,175 live births). The median age of first symptoms was 21 years (range 10–33 years), and the median diagnostic delay was 10.5 years (range 0–29 years). The main clinical symptoms at the time of manifestation were stammering or slurred speech, proximal weakness of the lower extremities due to anterior horn cell neuronopathy, signs of neo- and paleocerebellar dysfunction and/or psychiatric disorders. Cerebellar atrophy detected through brain MRI was a common finding. Residual enzyme activity was 1.8–4.1% of controls. All patients carried the typical LOTS-associated c.805G>A (p.Gly269Ser) mutation on at least one allele, while a novel point mutation, c.754C>T (p.Arg252Cys) was found in two siblings.

Conclusion LOTS seems to be an underdiagnosed cause of progressive distal motor neuron disease, with variably expressed cerebellar impairment and psychiatric symptomatology in our group of adolescent and adult patients. The enzyme assay of β-hexosaminidase A in serum/plasma is a rapid and reliable tool to verify clinical suspicions.

Keywords Late-onset Tay–Sachs disease · GM2 gangliosidosis · β-Hexosaminidase A · Ataxia · Cerebellum · Proximal weakness of lower extremities

Introduction

Tay–Sachs disease (TSD, OMIM 272800, 606869) is one of three neurodegenerative disorders caused by the intralysosomal storage of a specific glycosphingolipid, GM2 ganglioside, in neurons. Physiologically, the degradation of GM2 ganglioside is performed by the intralysosomal enzymes β-hexosaminidase A (HexA) and β-hexosaminidase B (HexB) in cooperation with a specific glycoprotein called GM2 activator. Both HexA and HexB are dimers. HexA is

✉ Martin Magner
martin.magner@vfn.cz

[1] Department of Paediatrics and Adolescent Medicine, First Faculty of Medicine, Charles University and General University Hospital in Prague, Ke Karlovu 2, 120 00 Prague 2, Czech Republic

[2] Department of Neurology, First Faculty of Medicine, Charles University and General University Hospital, Prague, Czech Republic

[3] Department of Neurology, Second Faculty of Medicine, Charles University and University Hospital Motol, Prague, Czech Republic

[4] Department of Paediatric Neurology, Second Faculty of Medicine, Charles University and University Hospital Motol, Prague, Czech Republic

[5] Department of Biology and Medical Genetics, Second Faculty of Medicine, Charles University and University Hospital Motol, Prague, Czech Republic

a heterodimer composed of subunit α, the product of the *HEXA* gene, and subunit β, the product of the *HEXB* gene. HexB is a homodimer containing two β subunits. TSD (the B variant of GM2 gangliosidosis) is characterized by very low or absent HexA activity in the serum, plasma, dried blood spot, white blood cells or other tissues from a symptomatic person in the presence of normal or elevated HexB activity. Mutations specific for TSD are present in the *HEXA* gene. Significantly decreased or absent activities of both HexA and HexB are typical for Sandhoff disease (the 0 variant of GM2 gangliosidosis), with associated mutations in the *HEXB* gene. In the very rare disorder GM2 activator deficiency (the AB variant of GM2 gangliosidosis), the enzyme activities of both HexA and HexB are normal with fluorogenic substrates [1, 2]. All three disorders have autosomal recessive inheritance.

TSD is classified into three subtypes according to the clinical course—an acute infantile (classic) form with rapid progression and death before the age of 4 years, a subacute juvenile form with onset in early childhood and longer survival, and a chronic adult/late-onset form (LOTS) with slow progression and long-term survival. While the infantile form is characterized by early and rapid neurodevelopmental regression, epileptic seizures and vision deterioration with a typical "cherry-red spot" caused by the accumulation of various sphingolipids within retinal cells [3], the main reported symptoms of LOTS are cerebellar and extrapyramidal signs, lower motor neurons impairment and variable psychiatric conditions [2].

The birth prevalence of the acute infantile form of TSD was originally very high in the Ashkenazi Jewish community (approximately 1:3600) and some other genetically isolated populations. The introduction of population-based carrier screening, education and counselling helped to decrease the frequency of infantile TSD patients in such endangered communities [4-6]. On the other hand, LOTS, which is not so tightly associated with the Ashkenazi Jewish community, has rarely been reported in the literature. A study of 21 patients with LOTS was published in the USA [7], but only 3 isolated case reports have been published in Europe [8-10]. A substantial number of LOTS patients may escape a correct diagnosis, as their clinical symptomatology significantly differs from the well-known picture of classic infantile TSD [7, 11]. Although an effective treatment for TSD is not available at present, evaluation of the occurrence and clinical manifestation of LOTS may be important for future progress in this field. Therefore, we present clinical phenotypes, laboratory data and mutation spectrums of 14 Czech patients with LOTS, diagnosed between the years 2002 and 2018.

Patients and methods

Patients

In all patients, final diagnoses of LOTS were performed in the Department of Paediatrics and former Institute of Inherited Metabolic Disorders of the First Faculty of Medicine, Charles University in Prague. Two patients were primarily revealed by clinical exome sequencing (CES) in the molecular genetic laboratory of the Department of Biology and Medical Genetics of the Second Faculty of Medicine, Charles University and University Hospital Motol in Prague. Brain MRI and electromyography/nerve conduction velocity (EMG/NCV) studies were conducted through neurologists who provided regular patient care. Clinical examinations were carried out by clinicians of the concerned institution in cooperation with individual patients' neurologists. To our knowledge, the reported 14 patients represent the absolute majority of Czech patients diagnosed with LOTS in the past 20 years.

Enzymology

For the determination of enzyme activities, serum, plasma and white blood cells were prepared by standard procedures. The activities of the lysosomal enzymes β-hexosaminidase A (*N*-acetyl-β-D-glucosaminidase A) and β-D-galactosidase (control enzyme) were determined by fluorometric methods using 4-methylumbelliferyl-6-sulpho-2-acetamido-2deoxy-β-D-glucopyranoside and 4-MU-β-D-galactopyranoside as substrates, respectively [12].

Molecular genetic analyses

Genomic DNA was isolated from blood. Mutation analysis in all but two patients was based on direct sequencing of PCR products for all coding exons (1 to 14) of the *HEXA* gene using a 3500xL Genetic Analyzer capillary sequencer (Applied Biosystems). Primer specifics and reaction conditions are available upon request. The DNA mutations are described according to actual *HEXA* reference DNA sequence [13] (nomenclature via HGVS recommendations) [14]. For the CES of two patients, a Focused Exome and SureSelect Reagent kit (Agilent Technologies) was used for clinical exome capture, and sequencing was performed with an Illumina HiSeq1500 system. The detected variants were confirmed by Sanger sequencing.

Ethics

All information were accessed in accordance with the applicable laws and ethical requirements for the study period concerned (in particular the Helsinki Declaration, revised in 2000). All patients signed informed consent with genetic testing. The study was approved by the Institutional Review Board of the General University Hospital in Prague (Ethics Committee Approval Number: 41/12).

Results

Study group

In total, 14 LOTS patients from 10 families, 9 females and 5 males, were included in the study (Table 1). All but one were diagnosed between the years 2011 and 2018. The median age of first symptoms was 21 (range 10–33 years), while the median age of the diagnostic assessment was 35 years (range 18–54 years), resulting in a median diagnostic delay of 10.5 (range 0–29 years). The calculated birth prevalence of LOTS for the Czech Republic (CR) is 1 per 325,175 live births and the calculated birth prevalence of all forms of TSD in the CR is 1 per 212,071 live births. No patient reported was of Jewish Ashkenazi ancestry. All but one patient are still alive; the first diagnosed patient (Table 1, Pt 6) died due to complications from a head injury.

Clinical manifestations

The main clinical findings are summarized in the Table 1 (initial complaints) and Table 2 (neuropsychiatric symptomatology).

Table 1 Onset of the disease, enzyme activity and mutations in the *HEXA* gene in 14 Czech patients with the late-onset form of Tay–Sachs disease

No	*G*	Age at onset (years)	First symptoms	Age at diagnosis (years)	Diagnostic delay (years)	Approx. Resid. Enzyme activity in L (%)	Mutations (gene *HEXA*), predicted effect on protein
1[a]	F	10	Slurred speech	30	20	2.2	c.805G>A/c.1123delG p.G269S/p.E375Rfs*7
2[a]	F	15	Slurred speech, proximal weakness (LE)	18	3	2.5	c.805G>A/c.1123delG p.G269S/p.E375Rfs*7
3	M	30	Cerebellar ataxia, falls, dysmetria, dysarthria	46	16	2.3	c.805G>A/c.1073 + 1G>A p.G269S/missplicing
4[a]	F	30	Depression, proximal weakness (LE), dysphonia	38	8	3.3	c.805G>A/c.1274_1277dupTATC p.G269S/p.Y427Ifs*5
5[a]	F	30	Depression, proximal weakness (LE), dysarthria	33	3	3.7	c.805G>A/c.1274_1277dupTATC p.G269S/p.Y427Ifs*5
6	M	18	Schizophrenia-like disorder	31	13	4.1	c.805G>A/c.806G>A p.G269S/p.G269D
7	M	33	Tremor, cerebellar ataxia, dysarthria	37	4	1.8	c.805G>A/c.805G>A p.G269S/p.G269S
8	F	20	Cerebellar ataxia, tremor, proximal weakness	45	25	2.4	c.805G>A/c.1274_1277dupTATC p.G296S/p.Y427Ifs*5
9	F	23	Cerebellar ataxia, proximal weakness (LE), tremor (UE)	38	15	2.6	c.805G>A/c.1123delG p.G269S/p.E375Rfs*7
10[a]	M	25	Proximal weakness (LE), falls, slurred speech	46	21	3.8	c.805G>A/c.754C>Tb p.G269S/p.R252Cb
11[a]	M	25	Proximal weakness (LE), slurred speech	54	29	3.5	c.805G>A/c.754C>Tb p.G269S/p.R252Cb
12[a]	F	17	Mild dysarthria, proximal weakness (LE), falls	24	7	3.3	c.805G>A/c.1274_1277dupTATC p.G296S/p.Y427Ifs*5
13[a]	F	17	Proximal weakness (LE), falls	20	3	3.7	c.805G>A/c.1274_1277dupTATC p.G296S/p.Y427Ifs*5
14	F	25	Dysarthria, proximal weakness (LE), tremor (UE)	25	0	2.9	c.805G>A/c.1073 + 1G>A p.G296S/missplicing

LE low extremities, *UE* upper extremities, *L* leukocytes, *F* female, *M* male

[a]Patients 1 and 2; 4 and 5; 10 and 11; 12 and 13 are siblings

[b]Mutation in siblings 10 and 11 is novel

Table 2 Neuropsychiatric symptomatology in the group of 14 Czech patients with late-onset form of Tay–Sachs disease

No.	Weakness and amyotrophy of LE	Anterior horn cells neuronopathy (based on EMG/NCV and clinical findings)	Dysmetria, action tremor of UE (neocerebellar syndrome)	Slurred speech, stammering, dysarthria	Cerebellar ataxia, gait instability (paleocerebellar syndrome)	Dystonia, dyskinesia	Pyramidal signs	Psychosis	Mild cognitive impairment	Cerebellar atrophy (MRI)
1	+	+	+	+	+	−	−	+	−	+
2	+	+	+	+	+	−	−	−	−	+
3	−	ND	+	+	+	−	−	−	−	+
4	+	+	−	+	−	+	−	+	+	+
5	+	+	−	+	−	+	−	+	+	+
6	−	ND	+	−	+	−	−	+	−	+
7	+	+	+	+	+	−	−	−	−	+
8	+	+	+	−	+	−	−	+	−	+
9	+	+	+	−	+	−	−	−	+	+
10	+	+	−	+	+	−	−	−	−	+
11	+	+	−	+	+	−	−	−	−	+
12	+	+	+	+	+	−	−	−	+	+
13	+	+	−	−	+	−	−	−	−	+
14	+	+	+	+	−	−	−	−	−	+

N number, *LE* lower extremities, *UE* upper extremities, *MRI* magnetic resonance imaging, *EMG* electromyography, *NCV* nerve conduction velocity, *ND* not done

Generally, the main initial complaints in the cohort were mild articulation difficulties, especially slurred rapid speech and/or stammering (nine patients), proximal weakness of the lower extremities limiting walking down and up the stairs (nine patients), dysmetria, action tremor and gait instability with frequent falls (eight patients), and/or schizophrenic and maniodepressive disorders (three patients). Some patients reported having been "a clumsy child", but others (three patients) participated in various sports during childhood and adolescence. No optic atrophy or "cherry-red spot" was described in any patient, but mild variable signs of oculomotoric dysfunction (gaze dyscoordination, mild saccade and pursuit irregularity) were present in some patients during clinical progression of the disease. Fluctuating horizontal nystagmus was present in one male (Pt 7). Some patients suffered from common myopia or hypermetropia. In one male (Pt 3), gait instability with frequent falls and severe dysmetria without significant weakness of the lower extremities (combined cerebellar syndrome) dominated. He had no nystagmus, nor any other ocular movement dysfunction. Organomegaly and/or cardiac disease were not found in any patient of the cohort.

In three patients, the first symptom of LOTS was a psychiatric disorder. In one male (Pt 6), acute schizophrenia-like disorder with relapses preceded the development of combined cerebellar symptomatology by 6 years. Schizoaffective disorder (predominantly depression) and weakness of the lower extremities were the first symptoms in two sisters (Pts 4 and 5). In another two females (Pts 1 and 8), severe episodes of maniodepressive disorder requiring psychopharmacologic treatment appeared about 10 years after manifestation of the first motor symptoms. Four other patients suffered from likely secondary moderate depressive symptomatology. All but one patient underwent at least one psychological examination; mild cognitive decline was assessed in four females, while in other patients, the overall cognitive level was normally distributed.

Mild dystonia/dyskinesia in two females (Pts 4 and 5) may have been partly due to neuroleptic treatment. No signs of pyramidal tract impairment were found in patients of the cohort.

In patients manifesting predominantly with proximal weakness of the lower extremities, results of complex neurological examinations corresponded to anterior horn cell damage. These patients had proximal and distal amyotrophy predominantly in the lower limbs without any sensory impairment. Fasciculations were noticed only rarely in some patients, less frequently in severely disabled persons. EMG/NCV studies were performed in 12 patients and documented chronic neurogenic lesion with reinnervation changes of motor unit potentials (MUPs), especially in the proximal muscles of lower extremities, corresponding to anterior horn cell neuronopathy.

Variably prominent lamellar cerebellar atrophy (in two females very mild) was found in brain MRI in all 14 patients.

Laboratory findings

Residual enzyme activities ranged between 1.8 and 4.1% of the control average; there were no significant differences in serum/plasma and leukocytes. The most frequent nucleotide expansion-based spinocerebellar ataxias (SCAs) were excluded by routine DNA analyses in six patients. Due to the clinical picture resembling spinal amyotrophy, DNA analysis of the *SMN1* gene was performed in ten patients with normal results, while the late-onset form of Pompe disease was excluded in five patients by an enzyme assay. The c.805G>A (p.Gly269Ser) mutation that is typically associated with LOTS [9] was found in all 14 patients, with 1 patient carrying this mutation on both alleles (Table 1, Fig. 1). In half of cases (7/14), a compound heterozygosity for c.805G>A and the previously described null mutation (c.1073+1G>A or c.1274_1277dup) were detected, while in another three cases, the c.805G>A mutation occurred along with the frameshift mutation c.1123delG. The remaining two patients were carriers of a previously unpublished missense mutation c.754C>T (p.Arg252Cys). One patient carried the mutation c.806G>A, which is the first nucleotide of exon 8 in the conserved splice domain (possibly inducing missplicing).

Discussion

LOTS is considered to be a very rare disease. However, in the Czech Republic, with 10.58 million inhabitants, 13 patients have been diagnosed in the last 8 years, which is in sharp contrast to only 3 isolated cases published by European authors so far [8-10]. From the genetic point of view, it is likely that the Czech population does not differ from other European countries substantially. We presume

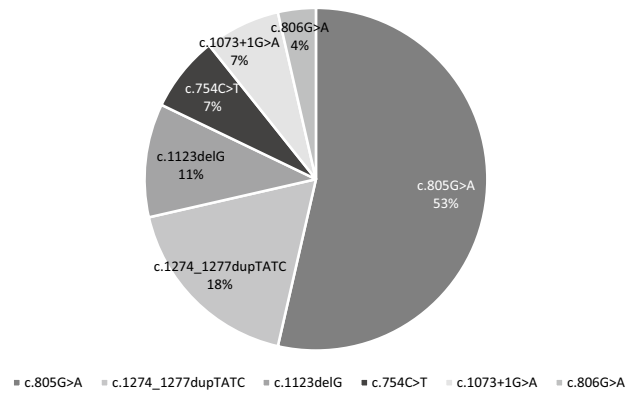

Fig. 1 Frequency of distinct mutations in the group of 14 Czech patients with the late-onset form of Tay–Sachs disease

that reasons for the apparent underdiagnosis of this disease, documented also by the long interval between age of onset and age of diagnosis, include both the quite different clinical symptomatology of LOTS in comparison with the infantile form TSD and the broad differential diagnostic spectrum of spinal muscular atrophy, motor axonal neuropathies, cerebellar disorders and psychiatric conditions.

Neurological clinical features of LOTS are variable, but slowly progressing symptoms of anterior horn cell neuronopathy especially at the lower extremities and cerebellar dysfunction (not necessarily simultaneously in one patient) are prominent. In accordance with literary sources, about half of patients in our cohort suffered from psychiatric disturbances including schizophrenia-like psychosis and depression, and in three persons these symptoms represented the first manifestation of LOTS. Psychiatric symptoms were sometimes atypical and bizarre, such as disorganized schizophrenia, catatonia, regression to childhood behaviour or conflicting personality disorder (as in Pt 6) [15, 16].

While amyotrophy of the lower limbs and cerebellar signs (dysmetria, action tremor, severe gait instability without sensory deficits, typical dysarthria) were frequent symptoms in our patients with LOTS, dystonia mentioned in the literature was found in only two females of our cohort. A partial effect of neuroleptic treatment could not be excluded. It is important to mention that falling in LOTS is often the result of "knee buckling" due to weakness of knee extensor muscles rather than due to ataxia. Only four of our patients suffered from mild cognitive impairment, though the possibility of a negative influence from reactive depression is not negligible. The absence of significant cognitive decline or dementia in our patients is in concordance with findings in a group of 21 American patients, and thus seems to be an important feature of LOTS [7]. The involvement of the eyes in some patients was minimal and unspecific. There was no optic nerve atrophy or finding of a “cherry-red spot” in our cohort. EMG/NCV findings indicating chronic anterior horn cell neuropathy and cerebellar atrophy in the brain MRI were typical clinical laboratory findings.

Based on our experience, the enzyme assay of β-hexosaminidase A in serum/plasma is a rapid, inexpensive and reliable tool to verify clinical suspicion, and we did not experience any false positive result in our Czech cohort. Similarly as in some other lysosomal disorders, β-hexosaminidase A activity assessment in serum/plasma/dried blood spot could serve as a possible screening method in the groups of clinically selected patients.

In line with literary data [17], the presence of the p.Gly269Ser (c.805G>A) allele in the *HEXA* gene responsible for incorrect enzyme dimer forming is typical for the adult form of the disease. Combinations with null alleles in our group of patients led to both a more complex symptomatology and a more progressive course of disease. In two brothers with the common c.805G>A mutation and the novel c.754C>T mutation, LOTS manifested in their 3rd decade, but the course was slow, with relatively mild weakness of the lower extremities, mild cerebellar symptomatology and normal cognitive functions.

Currently, there is no effective treatment for LOTS and management is only supportive, but several treatment strategies have been tested. Although bone marrow transplantation led to stabilisation of the disease in a 15-year-old boy [18], the therapeutic effect is generally considered to be minimal [19]. Intrathecal infusion of the pure β-hexosaminidase A was tested in two patients with the infantile form TSD with no benefit [20]. Substrate reduction therapy with miglustat or chaperone therapy with pyrimethamine likewise showed no clinical benefits [21, 22]. While the results of these studies are still not satisfactory, we strongly believe that a higher number of diagnosed patients may enhance research for effective treatment.

Conclusion

Though the individual clinical course of disease is variable, the combination of slowly progressive anterior horn cell neuronopathy manifesting mostly at the lower extremities, with variably expressed cerebellar symptomatology and corresponding cerebellar atrophy in the brain MRI should direct clinicians´ suspicion to LOTS, especially if episodes of psychotic behaviour occur simultaneously. A serum/plasma enzyme assay of beta-hexosaminidase A activity is an inexpensive and reliable primary diagnostic tool. We hope that the increased number of diagnosed patients will support efforts in the search for effective treatments.

Acknowledgements The work was supported by the Grant UNCE 204064; PROGRES Q26/LF1 and RVO-VFN 64165/2012.

Compliance with ethical standards

Conflicts of interest The authors declare that they have no conflict of interest.

References

1. Gravel RA, Kaback MM, Proia RL, et al (2014) The GM2 Gangliosidoses. In: The online metabolic and molecular bases of inherited diseases
2. Kaback MM, Desnick RJ (2011) Hexosaminidase A deficiency. In: Pagon R, Adam M (eds) GenReviews, pp 1993–2018
3. Chen H, Chan AY, Stone DU, Mandal NA (2014) Beyond the cherry-red spot: Ocular manifestations of sphingolipid-mediated neurodegenerative and inflammatory disorders. Surv. Ophthalmol. 59:64–76
4. Kaback M, Lim-Steele J, Dabholkar D et al (1994) Tay–Sachs disease—carrier screening, prenatal diagnosis and the molecular

era: an international perspective, 1970 to 1993. Obstet Gynecol Surv 270:2307–2315. https://doi.org/10.1097/00006254-199405000-00013
5. Kaback MM (2000) Population-based genetic screening for reproductive counseling: the Tay–Sachs disease model. Eur J Pediatr 159:192–195. https://doi.org/10.1007/PL00014401
6. Scott SA, Edelmann L, Liu L et al (2010) Experience with carrier screening and prenatal diagnosis for 16 Ashkenazi Jewish genetic diseases. Hum Mutat 31:1240–1250. https://doi.org/10.1002/humu.21327
7. Neudorfer O, Pastores GM, Zeng BJ et al (2005) Late-onset Tay–Sachs disease: phenotypic characterization and genotypic correlation in 21 affected patients. Genet Med 7:119–123
8. Steiner KM, Brenck J, Goericke S, Timmann D (2016) Cerebellar atrophy and muscle weakness: late-onset Tay–Sachs disease outside Jewish populations. BMJ Case Rep 31:5
9. Barritt AW, Anderson SJ, Leigh PN, Ridha BH (2017) Late-onset Tay–Sachs disease. Pract Neurol 17:396–399. https://doi.org/10.1136/practneurol-2017-001665
10. Prihodova I, Kalincik T, Poupetova H et al (2013) Late-onset Tay–Sachs disease can mimic spinal muscular atrophy type III—two case reports. Ces a Slov Neurol a Neurochir 76:221–224
11. Navon R, Argov Z, Frisch A (1986) Hexosaminidase A deficiency in adults. Am J Med Genet 24:179–196. https://doi.org/10.1002/ajmg.1320240123
12. Wenger D, Williams C (1991) Screening for lysosomal disorders. In: Hommes FA (ed) Techniques in diagnostic human biochemical genetics. Willey-Liss, New York, pp 587–617
13. HEXA hexosaminidase subunit alpha [Homo sapiens (human)]. https://www.ncbi.nlm.nih.gov/gene/3073. Accessed 30 Sep 2018
14. Human genom variation society. https://www.hgvs.org/. Accessed 17 Sep 2018
15. Streifler J, Golomb M, Gadoth N (1989) Psychiatric features of adult GM2gangliosidosis. Br J Psychiatry 155:410–413. https://doi.org/10.1192/bjp.155.3.410
16. MacQueen GM, Rosebush PI, Mazurek MF (1998) Neuropsychiatric aspects of the adult variant of Tay–Sachs disease. J Neuropsychiatry Clin Neurosci 10:10–19. https://doi.org/10.1176/jnp.10.1.10
17. Navon R, Proia RL (1989) The mutations in Ashkenazi Jews with adult GM2gangliosidosis, the adult form of Tay–Sachs disease. Science 243:1471–1474. https://doi.org/10.1126/science.2522679
18. Stepien KM, Lum SH, Wraith JE et al (2017) Haematopoietic stem cell transplantation arrests the progression of neurodegenerative disease in late-onset Tay–Sachs disease. JIMD Rep 41:17–23. https://doi.org/10.1007/8904_2017_76
19. Neudorfer O, Kolodny EH (2004) Late-onset Tay–Sachs disease. Isr Med Assoc J 6:107–111
20. von Specht BU, Geiger B, Arnon R et al (1979) Enzyme replacement in Tay–Sachs disease. Neurology 29:848–854. https://doi.org/10.1212/WNL.29.6.848
21. Shapiro BE, Pastores GM, Gianutsos J et al (2009) Miglustat in late-onset Tay–Sachs disease: a 12-month, randomized, controlled clinical study with 24 months of extended treatment. Genet Med 11:425–433. https://doi.org/10.1097/GIM.0b013e3181a1b5c5
22. Osher E, Fattal-Valevski A, Sagie L et al (2015) Effect of cyclic, low dose pyrimethamine treatment in patients with Late Onset Tay Sachs: an open label, extended pilot study. Orphanet J Rare Dis 17:10–45. https://doi.org/10.1186/s13023-015-0260-7

Neurological Sciences
https://doi.org/10.1007/s10072-021-05757-3

ORIGINAL ARTICLE

Pontocerebellar atrophy is the hallmark neuroradiological finding in late-onset Tay-Sachs disease

Jitka Májovská[1] · Anita Hennig[2] · Igor Nestrasil[3] · Susanne A. Schneider[2] · Helena Jahnová[1] · Manuela Vaněčková[4] · Martin Magner[1,5] · Petr Dušek[4,6]

Received: 19 July 2021 / Accepted: 15 November 2021

Abstract

Purpose Late-onset Tay-Sachs disease (LOTS) is a form of GM2 gangliosidosis, an autosomal recessive neurodegenerative disorder characterized by slowly progressive cerebellar ataxia, lower motor neuron disease, and psychiatric impairment due to mutations in the *HEXA* gene. The aim of our work was to identify the characteristic brain MRI findings in this presumably underdiagnosed disease.

Methods Clinical data and MRI findings from 16 patients (10F/6 M) with LOTS from two centers were independently assessed by two readers and compared to 16 age- and sex-related controls.

Results Lower motor neuron disease (94%), psychiatric symptoms—psychosis (31%), cognitive impairment (38%) and depression (25%)—and symptoms of cerebellar impairment including dysarthria (94%), ataxia (81%) and tremor (69%), were the most common clinical features. On MRI, pontocerebellar atrophy was a constant finding. Compared to controls, LOTS patients had smaller mean middle cerebellar peduncle diameter ($p < 0.0001$), mean superior cerebellar peduncle diameter ($p = 0.0002$), mesencephalon sagittal area ($p = 0.0002$), pons sagittal area ($p < 0.0001$), and larger 4th ventricle transversal diameter ($p < 0.0001$). Mild corpus callosum thinning (37.5%), mild cortical atrophy (18.8%), and white matter T2 hyperintensities (12.5%) were also present.

Conclusion Given the characteristic clinical course and MRI findings of the pontocerebellar atrophy, late-onset Tay-Sachs disease should be considered in the differential diagnosis of adult-onset cerebellar ataxias.

Keywords Late-onset Tay-Sachs disease · Ataxia · Cerebellar atrophy · GM2 gangliosidosis · *HEXA* gene

Introduction

Tay-Sachs disease (OMIM #272,800), a form of GM2 gangliosidosis, is an autosomal recessive lysosomal neurodegenerative disorder caused by mutation in the *HEXA* gene. Dysfunction of the encoded enzyme beta-hexosaminidase A leads to intra-lysosomal accumulation of glycosphingolipid GM2 ganglioside in neurons. According to the clinical course, Tay-Sachs disease is classified into three subtypes—the acute infantile form, and the subacute juvenile and chronic adult forms that are also referred to as late-onset form of Tay-Sachs disease (LOTS). The infantile form is clinically characterized by progressive neurodevelopmental regression, hypotonia, epilepsy, blindness with the typical finding of a cherry-red spot in the retina, spasticity and early death before the age of four. LOTS is characterized by later onset of clinical symptoms and slower progression [1]. The typical manifestation of LOTS includes slowly progressive

✉ Petr Dušek
pdusek@gmail.com

1 Department of Pediatrics and Inherited Metabolic Disorders, First Faculty of Medicine, Charles University and General University Hospital, Prague, Czech Republic

2 Department of Neurology, Ludwig-Maximilians University, Munich, Germany

3 Department of Pediatrics, University of Minnesota, Minneapolis, MN, USA

4 Department of Radiology, First Faculty of Medicine, Charles University and General University Hospital, Prague, Czech Republic

5 Department of Pediatrics, University Thomayer Hospital and First Faculty of Medicine, Charles University, Prague, Czech Republic

6 Department of Neurology and Center of Clinical Neuroscience, First Faculty of Medicine, Charles University and General University Hospital, Prague, Czech Republic

Published online: 20 November 2021

symptoms of distal motor neuron lesion, cerebellar dysfunction, and psychiatric impairment. The calculated prevalence of LOTS in the Czech Republic is 1 per 325,175 live births [2] and it is believed that LOTS is underdiagnosed due to the slowly progressive disease course with psychiatric manifestation often preceding neurologic symptoms [2, 3].

Although the diagnosis is nowadays confirmed by genetic analysis, high clinical suspicion based on clinical manifestation and neuroimaging findings is necessary, particularly when whole exome sequencing is not readily available. The differential diagnosis includes motor neuropathies and spinocerebellar ataxias. Neuroimaging has proven to be partly helpful in the diagnosis due to the frequent finding of profound cerebellar atrophy without other conspicuous abnormalities in LOTS [3–14]. Other unspecific abnormalities such as thinning of the corpus callosum or gyral atrophy were also reported in some cases [4].

It was advocated that neuroimaging classification of cerebellar disorders according to the pattern of atrophy may assist in the clinical diagnostic process [15]. Specifically, three subtypes of cerebellar atrophy that follow classical neuropathological descriptions were suggested: spinal atrophy, cortical cerebellar atrophy, and (olivo)pontocerebellar atrophy. To date, no study assessed quantitative parameters and/or performed subtyping of cerebellar atrophy in LOTS.

Here, we aimed at describing characteristic brain MRI findings in LOTS with particular attention to semiquantitative measures of cerebellar and brainstem atrophy.

Patients and methods

Study participants

In this retrospective study, 16 patients from 13 families with a genetically confirmed diagnosis of LOTS and at least one brain MRI examination were included. None of the patients was of Jewish Ashkenazi descent. Patients were recruited from two centers—the Department of Paediatrics and Inherited Metabolic Disorders, General University Hospital and First Faculty of Medicine at the Charles University, Prague, Czech Republic ($n = 14$), and the Department of Neurology, Ludwig-Maximilians University, Munich, Germany ($n = 2$). Clinical data of 11 Czech patients have been reported in a previous study [2]. Sixteen sex- and age-comparable control subjects who underwent MRI as part of differential diagnosis process due to headache were included.

MRI parameters and assessment

Altogether, 32 MRI datasets were assessed. Twenty-one MRI exams were performed on 1.5 T and 11 MRI exams on 3 T scanners. All MRI datasets included standard clinical axial T1 weighted, T2 weighted, and fluid-attenuated inversion recovery (FLAIR) images. In each MRI dataset sagittal T1 weighted or FLAIR image was available. Control MRI datasets had normal MRI finding and pulse sequence parameters comparable to those of LOTS patients.

Several predefined markers were independently assessed by two raters (PD, JM): presence of pons vertical line/hot cross bun sign, severity of cerebellar cortical atrophy, transversal (latero-lateral) diameter of 4th ventricle, diameters of superior cerebellar peduncle (SCP) and middle cerebellar peduncle (MCP) from both sides, mid-sagittal area of midbrain, pons and medulla oblongata. Midbrain, pons, and medulla oblongata areas were manually delineated according to an adapted, previously described procedure [16, 17]. Brain MR assessments including semiquantitative measures are exemplified in Fig. 1. For SCP and MCP, mean values from the right and left side were used for analysis. Cerebellar cortical atrophy was scored on the four-point scale as absent (-), mild (+), moderate (++), and severe (+++). The assessment of cerebellar atrophy was based on the degree of thinning of the cerebellar folia, widening of the cerebellar fissures and subarachnoid spaces in the posterior fossa (Fig. 2). Supratentorial structures and skull were also systematically analyzed and presence of cortical or central atrophy, corpus callosum thinning, signal changes of the brain parenchyma as well as dural thickening, craniocervical junction abnormalities, sinus hypoplasia and mucosal thickening were noted for each subject. Discrepancy in the assessment were solved out through inter-rater discussion.

Clinical findings

Medical history and physical examination were retrospectively obtained from medical records. The following clinical data were evaluated: tremor, dysarthria, ataxia, dystonia, proximal leg weakness, depression, psychosis, and cognitive impairment.

Statistical analyses

Differences between patients with LOTS and control groups were performed using univariate general linear model with the group as a fixed factor and age and sex as covariates. Agreement between raters was evaluated using intraclass correlation coefficient. Spearman's rank correlation coefficient was calculated to assess the associations between disease duration and MRI parameters. P-values of < 0.05, corrected for multiple comparisons using the Holm-Bonferroni method, were considered statistically significant. IBM SPSS statistics version 25 (IBM, Armonk, NY, USA) was used

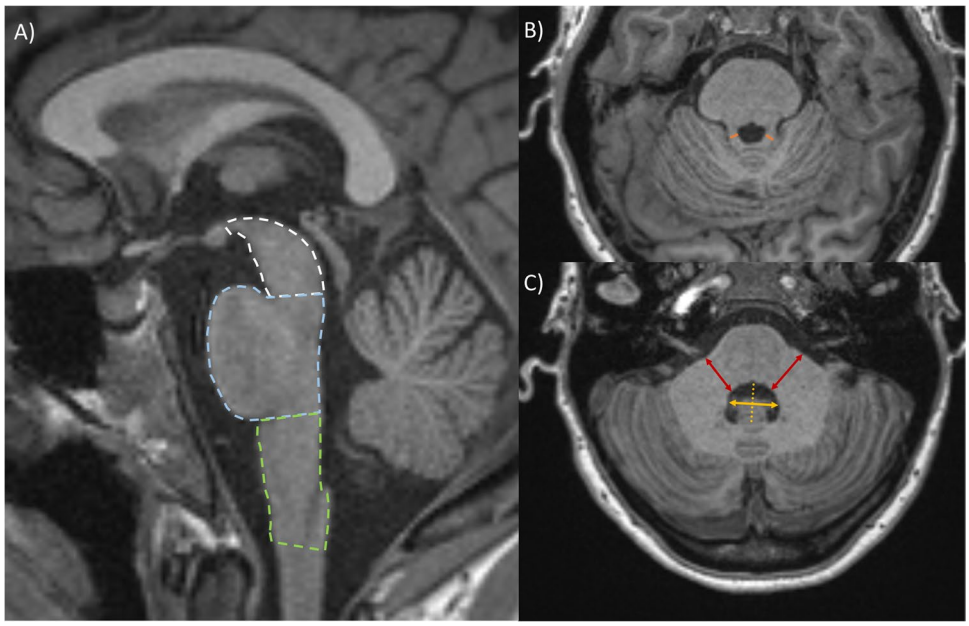

Fig. 1 Assessment of brain MR images. A) Representative midsagittal T1-weighted image in a control subject. Midbrain, pons, and medulla oblongata areas were delineated manually according to the method described by Oba et al. [16] and Reetz et al. [17]. In short, the caudal edge of midbrain was defined as line passing through the superior pontine notch and the inferior edge of the quadrigeminal plate; caudal edge of pons was defined as a line parallel to the first line passing through the inferior pontine notch; caudal edge of medulla oblongata was delimited along the foramen magnum. The area of the midbrain (excluding the tectum) was traced above the first line (outlined as white dashed line). The area of the pons was traced between the first and second line (outlined as blue dashed line). The medulla oblongata was traced between the second and third line (outlined as green dashed line). Representative axial T1-weighted images at the level of B) superior and C) middle cerebellar peduncles in a healthy control. Diameter of superior cerebellar peduncles (orange lines) was measured in the middle between cerebellum and midbrain. Diameter of 4th ventricle (yellow line) was measured in an axial slice where its latero-lateral size was largest; the measurement was performed in the middle of antero-posterior diameter of the ventricle (yellow dashed line). Diameter of middle cerebellar peduncles was measured at the same slice as 4th ventricle perpendicularly to the anterior boundary of the peduncle (red lines)

for statistical analysis; graphs were plotted using Prism 8 (GraphPad Software, San Diego, CA, USA).

Ethics

All information was accessed in accordance with the applicable laws and ethical requirements for the study period concerned in compliance with the Declaration of Helsinki, revised in 2013. All examined patients signed an informed consent form for genetic testing. The study was approved by the Institutional Review Board of the General University Hospital in Prague (Ethic Committee Approval Number 1471/19).

Results

Patient characteristics

Clinical data of 16 patients (10 females, 6 males) are summarized in Table 1. The median age at symptom onset was 21.5 years (range 6–33 years) and the median diagnostic delay was 12.5 years (range (0–31 years)). The median age at the last brain MRI exam that was used for the analysis in this study was 34.5 years (range 17–54 years). The median time gap between brain MRI and neurological examinations in a specialized center was 0.5 (range 0–9) years.

Proximal leg weakness was present in 15/16 patients (94%), other neurological symptoms included dysarthria (15/16; 94%), ataxia (13/16; 81%), tremor (11/16; 69%), and dystonia (3/16; 19%). The most common psychiatric symptoms were psychosis (5/16; 31%), cognitive impairment (6/16; 38%), and depression (4/16; 25%).

MRI datasets were available for 16 age- and sex-matched controls (10 females, 6 males, median age at the time of MRI exam was 34, range 18–53 years).

MRI findings

Between-rater agreement for semi-quantitative measures of brainstem and cerebellar atrophy was good to excellent with intraclass correlation coefficient values ranging from 0.80 to 0.97 (Table 2).

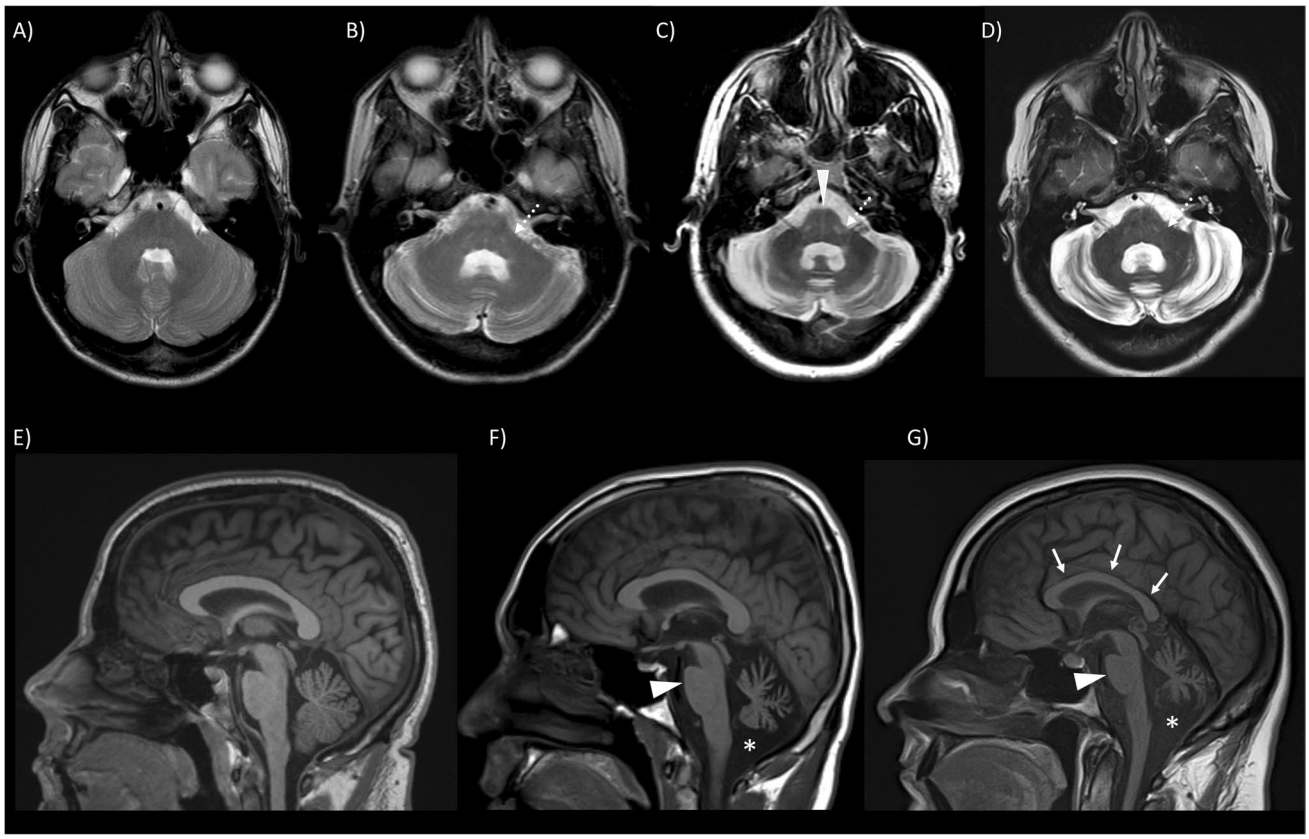

Fig. 2 Brain MRI findings in late-onset Tay-Sachs disease. Representative axial T2-weighted images at the level of the 4th ventricle in A) control subject, and LOTS patients with B) mild, C) moderate, D) severe cerebellar cortical atrophy. Note that the 4th ventricle is enlarged and the middle cerebellar peduncle is atrophic (dotted white arrows) in all LOTS patients regardless of the degree of cerebellar cortical atrophy. Vertical line in the pons (white arrowhead) is apparent in C). Sagittal T1-weighted images of E) healthy control and LOTS patients with F) moderate, and G) severe cerebellar cortical atrophy. Note the enlargement of cisterna magna (asterisk) and antero-posterior flattening of the pons (white arrowheads) in both patients. Mild thinning of corpus callosum (white arrows) is apparent in G)

Brain MRI findings of patients are summarized in Table 1 and comparison with controls in Table 2.

Vertical line in the pons was observed in three patients (19%) (Fig. 2) while the hot cross bun sign was not noted in any subject. Cerebellar cortical atrophy was present in all patients; it was rated as mild in one (6%), moderate in six (38%), and severe in nine (56%) patients.

Compared to controls, LOTS patients had significantly smaller mean MCP diameter ($p < 0.0001$), mean SCP diameter ($p = 0.0002$), mesencephalon sagittal area ($p = 0.002$), pons sagittal area ($p < 0.0001$), and larger 4th ventricle transversal diameter ($p < 0.0001$) (Table 2). Pons sagittal area in 11 (69%) and MCP diameter in 15 (94%) LOTS patients was lower than in any control subject. With the cutoff 1.7 cm, there was no overlap in 4th ventricle transversal diameter between LOTS patients and controls (Fig. 3).

We found no correlation between the degree of cerebellar atrophy and clinical symptoms; e.g., two patients (number 9, 11) with moderate to severe cerebellar cortical atrophy were free of cerebellar ataxia (Table 1). We also found no associations between disease duration and 4th ventricle transversal diameter, SCP or MCP diameters, sagittal areas of mesencephalon, pons or medulla oblongata, and cerebellar cortical atrophy score.

Mild corpus callosum thinning was seen in six patients (38%) and mild cortical atrophy in three patients (19%). Abnormalities in supratentorial signal intensity were observed in two patients (13%)—one patient had left frontal periventricular white matter T2 hyperintensity, the other had right frontal deep white matter T2 hyperintensity. Abnormal signal in the deep grey matter and skull abnormalities were not observed in any patient.

Discussion

We performed a retrospective analysis of routine clinical brain MRI in 16 LOTS patients in order to identify and describe characteristic imaging features. In contrast to

Table 1 Clinical and neuroimaging findings in patients with adult form of Tay-Sachs disease

	Gender	Age at onset (years)	Age at diagnosis (years)	Age at the time of MRI	Current age (years)	Diagnostic delay (years)	*HEXA* mutation	Clinical findings								MRI findings		
								Tremor	Dysarthria	Ataxia	Dystonia	Proximal lower limb weakness	Depression	Psychosis	Cognitive impairment	Hot cross bun sign/ vertical line	Cerebellar atrophy	Other findings
Patient 1	M	30	46	43	53	16	c.805G > A/c.1073 + 1G > A p.G269S/ missplicing	+	+	+	-	-	+	-	-	VL	+++	Mild CC thinning
Patient 2[a]	F	10	30	29	39	20	c.805G > A/c.1123delG p.G269S/p.E375Rfs*7	+	+	+	-	+	-	+	-	-	++	Left frontal periventricular WM T2 hyperintensity
Patient 3[a]	F	15	18	17	28	3	c.805G > A/c.1123delG p.G269S/p.E375Rfs*7	+	+	+	-	+	-	-	-	-	+	-
Patient 4	M	20	30	30	41	10	c.805G > A/c.1274_1277dupTATC p.G269S//p.Y427Ifs*5	+	+	+	-	+	+	-	-	-	+++	-
Patient 5[b]	M	25	46	49	51	21	c.805G > A/c.754C > T p.G269S/p.R252C	-	+	+	-	+	-	-	+	-	+++	-
Patient 6[b]	M	25	54	54	56	29	c.805G > A/c.754C > T p.G269S/p.R252C	-	-	+	-	+	-	-	-	-	+++	Mild cortical atrophy
Patient 7	M	33	37	37	43	4	c.805G > A/c.805G > A p.G269S/p.G269S	+	+	+	-	+	-	-	-	-	+++	Mild cortical atrophy
Patient 8	F	19	42	39	45	23	c.805G > A/c.1444G > A p.G269S/p.E482K	-	+	+	-	+	-	+	-	-	+++	Mild CC thinning
Patient 9[c]	F	30	38	38	46	8	c.805G > A/c.1274_1277dupTATC p.G269S/p.Y427Ifs*5	-	+	-	+	+	-	+	+	-	++	-
Patient 10	F	25	25	28	31	0	c.805G > A/c.1073 + 1G > A p.G296S/ missplicing?	+	+	-	-	+	+	-	-	-	++	-
Patient 11[c]	F	30	33	35	40	3	c.805G > A/c.1274_1277dupTATC p.G269S/p.Y427Ifs*5	-	+	-	+	+	-	+	+	-	+++	Right frontal deep WM T2 hyperintensity
Patient 12	F	17	24	21	28	7	c.805G > A/c.1274_1277dupTATC p.G269S/p.Y427Ifs*5	+	+	+	-	+	+	-	+	VL	++	-
Patient 13	F	12	42	41	42	30	c.805G > A/c.1330 + 1G > A p.G269S/ missplicing	+	+	+	-	+	-	-	-	-	+++	Mild CC thinning
Patient 14	F	23	38	28	43	15	c.805G > A/c.1123delG p.G269S/p.E375Rfs*7	+	+	+	-	+	-	-	+	-	++	Mild CC thinning
Patient 15	F	6	37	34	39	31	c.805G > A/ c.1073 + 1G > A p.G269S/ missplicing?	+	+	+	-	+	-	+	+	VL	++	Mild CC thinning

Table 1 (continued)

	Gender	Age at onset (years)	Age at diagnosis (years)	Age at the time of MRI	Current age (years)	Diagnostic delay (years)	*HEXA* mutation	Clinical findings								MRI findings		
								Tremor	Dysarthria	Ataxia	Dystonia	Proximal lower limb weakness	Depression	Psychosis	Cognitive impairment	Hot cross bun sign/vertical line	Cerebellar atrophy	Other findings
Patient 16	M	16	25	28	29	9	c.805G > A/c.947dupA p.G269S/pT316 *	+	+	+	+	+	-	-	-	-	+ + +	Mild CC thinning, mild cortical atrophy

M male, *F* female, [a]Patients 2 and 3 are siblings; [b]patients 5 and 6 are siblings, [c]Patients 9 and 11 are siblings, *VL* vertical line, *CC* corpus callosum, *WM* white matter

previous reports of absent brainstem atrophy [4, 5, 7, 11, 12], we found pontocerebellar atrophy to be the hallmark of LOTS in our study. In three patients, pontine atrophy was accompanied by vertical line in the pons, features also recognized in the cerebellar type of multiple system atrophy and several spinocerebellar ataxias [18]. Prominent atrophy of cerebellum, pons and middle cerebellar peduncles underlay the enlargement of the 4th ventricle that was a common finding in all patients. Additionally, we have found atrophy of mesencephalon and SCP although it was not consistent and its effect size was notably smaller compared to pontine and MCP atrophy. While pontocerebellar atrophy is an unspecific finding that is present in several sporadic and hereditary disorders such as multiple system atrophy, autosomal dominant spinocerebellar ataxias [19], or fatty acid hydroxylase-associated neurodegeneration [20], it may help to narrow down the differential diagnosis and distinguish LOTS from ataxias with predominant spinal or cerebellar cortical atrophy such as Friedreich ataxia and other autosomal recessive cerebellar ataxias, or paraneoplastic/ autoimmune cerebellar degenerations [21].

Mild thinning of the corpus callosum was found in 38% of patients, similarly to the study of Streifler et al. [4], which described thinning of the corpus callosum in five out of ten patients. The specificity of corpus callosum thinning is low due to its presence in a variety of disorders including leukoencephalopathies, metabolic disorders, microcephaly, hydrocephalus, fetal alcohol syndrome, trauma and others [22].

Mild cortical atrophy was described in 19% of patients. Notably, none of these patients had cognitive impairment. Marked frontal atrophy that was previously reported [23] was not seen in any of our patients. Supratentorial abnormalities of signal intensity were seen only in two patients, which suggests that this finding may not be related to LOTS and is rather coincidental. Abnormal signals in the corticospinal tract [24] were not noted in any patient.

Clinical course of LOTS is highly variable. In line with the literature, cerebellar signs (ataxia, tremor, dysarthria) together with proximal leg weakness and psychiatric symptoms were the most common manifestation in our cohort [3, 6, 7, 25]. Cerebellar cortical atrophy is a constant neuroradiological finding in LOTS patients that is also visible in CT images [4, 10, 26]. Cerebellar atrophy was described even in patients without ataxia suggesting that cerebellar atrophy precedes clinical symptoms [4]. Accordingly, there was no correlation between severity of cerebellar atrophy and clinical symptoms in our group of patients. Additionally, no associations between disease duration and any MRI parameter were found in our study confirming that pontine and cerebellar atrophy is present early in the disease course. This is likely a consequence of very slow and individually variable disease progression as well as of differences in the

Table 2 Comparison of MRI measurements in patients with late-onset Tay Sachs disease and controls

	LOTS patients Mean (SD)	Controls Mean (SD)	*p*-value*	Effect size [Cohen's D]	Inter-rater agreement [ICC]
MCP average (mm)	13.06 (1.12)	16.45 (1.55)	**< 0.0001 (< 0.0001)**	2.5	0.97
SCP average (mm)	1.87 (0.24)	2.35 (0.45)	**0.0002 (0.0008)**	1.3	0.83
4th ventricle transversal diameter (mm)	23.22 (3.03)	14.44 (1.22)	**< 0.0001 (< 0.0001)**	3.8	0.97
Mesencephalon sagittal area (cm^2)	1.67 (0.13)	1.85 (0.18)	**0.002 (0.0033)**	1.1	0.80
Pons sagittal area (cm^2)	4.66 (0.43)	5.73 (0.55)	**< 0.0001 (< 0.0001)**	2.2	0.94
Medulla oblongata sagittal area (cm^2)	2.65 (0.23)	2.61 (0.26)	0.555 (0.5797)	0.2	0.95

LOTS late-onset Tay Sachs disease, *SD* standard deviation, *MCP* middle cerebellar peduncle, *SCP* superior cerebellar peduncle, *ICC* intraclass correlation coefficient

*p-values are adjusted for age, sex (unadjusted values are shown in brackets). Significant p-values after Holm-Bonferroni correction are shown in bold

brainstem and cerebellar degeneration during the prodromal phase. On the other hand, unreliable patient-reported age of disease onset due to different individual thresholds for perceiving neurological symptoms may also contribute to this finding.

Interestingly, the involvement of the cerebellum is common in lysosomal storage disorders. The pathophysiology of the primary cerebellar degeneration affecting many lysosomal storage disorders can likely be explained by the increased vulnerability of Purkinje cells triggered by accumulation of metabolic substrates [28]. Cerebellar atrophy as the neuroimaging hallmark has been reported in neuronal ceroid lipofuscinosis—especially the late onset and juvenile forms, Niemann-Pick disease type C, Gaucher disease, and Sandhoff disease [27, 28]. Neuroimaging findings often overlap. Therefore, the knowledge of other, more specific, markers is important. In patients with neuronal ceroid lipofuscinosis, other typical findings include cerebral atrophy, T2 hypointensity and T1 hyperintensity in the thalami and periventricular white matter abnormalities [29, 30]. Cerebellar atrophy is accompanied by cerebral atrophy, thinning of the corpus callosum, and increased signal in the periventricular white matter in Niemann-Pick disease type C [26] and by dural thickening in Gaucher disease [28, 31]. Cerebellar atrophy as a secondary finding can accompany other disorders like metachromatic leukodystrophy [28], or alpha-mannosidosis [32].

With regard to clinical phenotype in our group of patients, dystonia was present in 19% of patients that is more frequent than in previous studies.[8, 23] Psychiatric manifestation can be the initial manifestation in some patients and overall occurs in 30 to 50% of patients with LOTS [33, 34]. The prevalence of psychiatric manifestation was 68%, which may be explained by the long disease duration in our patient's group.

There are several limitations of the study. First, it is the small samples size, inherent to the rarity of this disorder, limiting strong conclusions and generalizability of the results. Due to a retrospective nature, brain MRI images were acquired on different scanners using non-identical pulse sequence parameters, which only allowed semi-quantitative assessments. Additionally, morphometric measurements were performed on routine clinical images and were not corrected for intracranial volume. Yet, differences in head size were not described in LOTS patients and controls were strictly sex-matched. Also, the statistical analyses were corrected for sex. Thus, the morphometric changes found in LOTS patients are trustworthy. Lastly, time gap between clinical and MRI examinations as well as the lack of quantitative assessment of clinical severity using validated scales are limiting factors for an accurate clinical-neuroimaging correlation.

In conclusion, profound pontocerebellar atrophy is the hallmark neuroradiological abnormality in patients with LOTS. This brain MRI feature is typical in other neurological disorders with resembling clinical symptoms such as spinocerebellar ataxias and multiple system atrophy. We propose that the concurrent presence of cerebellar symptoms and neuroradiological finding of pontocerebellar atrophy imply that LOTS should be considered the differential diagnosis of adult-onset cerebellar ataxias. In particular, the diagnosis of LOTS should be considered in cases where cerebellar signs are combined with lower motor neuron disease and psychiatric symptoms.

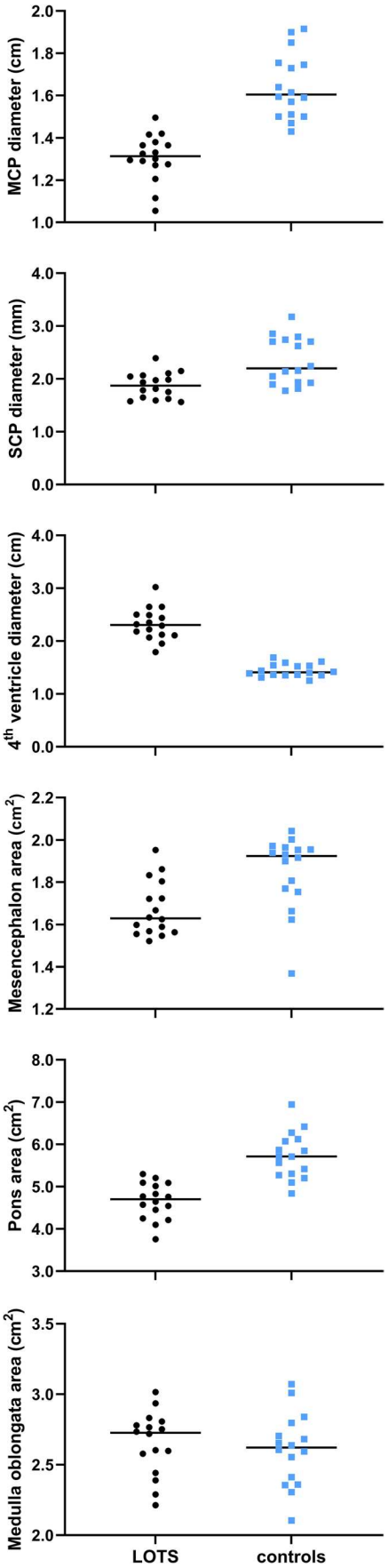

Fig. 3 Scatter plots of semiquantitative MRI measurements in patients with late-onset Tay Sachs disease and controls. Scatter plots of individual values in LOTS patients are on the left (black circles) and in controls on the right (blue rectangles). **LOTS** late-onset Tay Sachs disease, **MCP** middle cerebellar peduncle, **SCP** superior cerebellar peduncle

Funding This study was supported by Czech Ministry of Health, grant Nr. RVO 64165. SAS was supported by the Stiftung Verum, the Ara Parseghian Medical Research Fund and the intramural Munich Clinician Scientist Programme. PD was funded by Czech Ministry of Health, grant No. NU21-04–00535, General University Hospital in Prague, grant No. 20-L-13, and European Union's Horizon 2020 research and innovation programme, grant No. 633190.

Data availability De-identified individual participant data that underlie the results reported in this article will be shared upon reasonable request to the corresponding authors coming from researchers who provide a methodologically sound proposal.

Declarations

Ethics approval The study was approved by the Institutional Review Board of the General University Hospital in Prague (Ethic Committee Approval Number 1471/19).

Informed consent Informed consent was obtained from all individual participants included in the study.

Conflict of interest The authors declare no competing interests.

References

1. Toro C, Shirvan L, Tifft C. HEXA Disorders. In: Adam MP, Ardinger HH, Pagon RA, Wallace SE, Bean LJH, Mirzaa G, et al., editors. GeneReviews((R)). Seattle (WA)1993.
2. Jahnova H, Poupetova H, Jireckova J, Vlaskova H, Kostalova E, Mazanec R et al (2019) Amyotrophy, cerebellar impairment and psychiatric disease are the main symptoms in a cohort of 14 Czech patients with the late-onset form of Tay-Sachs disease. J Neurol 266(8):1953–1959
3. Neudorfer O, Pastores GM, Zeng BJ, Gianutsos J, Zaroff CM, Kolodny EH (2005) Late-onset Tay-Sachs disease: phenotypic characterization and genotypic correlations in 21 affected patients. Genet Med 7(2):119–123
4. Streifler JY, Gornish M, Hadar H, Gadoth N (1993) Brain imaging in late-onset GM2 gangliosidosis. Neurology 43(10):2055–2058
5. Steiner KM, Brenck J, Goericke S, Timmann D. Cerebellar atrophy and muscle weakness: late-onset Tay-Sachs disease outside Jewish populations. BMJ Case Rep. 2016;2016.
6. Mitsumoto H, Sliman RJ, Schafer IA, Sternick CS, Kaufman B, Wilbourn A et al (1985) Motor neuron disease and adult hexosaminidase A deficiency in two families: evidence for multisystem degeneration. Ann Neurol 17(4):378–385
7. Hund E, Grau A, Fogel W, Forsting M, Cantz M, Kustermann-Kuhn B et al (1997) Progressive cerebellar ataxia, proximal neurogenic weakness and ocular motor disturbances: hexosaminidase A deficiency with late clinical onset in four siblings. J Neurol Sci 145(1):25–31

8. Jamrozik Z, Lugowska A, Golebiowski M, Krolicki L, Maczewska J, Kuzma-Kozakiewicz M (2013) Late onset GM2 gangliosidosis mimicking spinal muscular atrophy. Gene 527(2):679–682
9. Inglese M, Nusbaum AO, Pastores GM, Gianutsos J, Kolodny EH, Gonen O (2005) MR imaging and proton spectroscopy of neuronal injury in late-onset GM2 gangliosidosis. AJNR Am J Neuroradiol 26(8):2037–2042
10. Streifler J, Golomb M, Gadoth N (1989) Psychiatric features of adult GM2 gangliosidosis. Br J Psychiatry 155:410–413
11. Barritt AW, Anderson SJ, Leigh PN, Ridha BH (2017) Late-onset Tay-Sachs disease. Pract Neurol 17(5):396–399
12. Deik A, Saunders-Pullman R (2014) Atypical presentation of late-onset Tay-Sachs disease. Muscle Nerve 49(5):768–771
13. Peters AS, Markovic K, Schramm A, Schwab S, Heuss D. Late onset hexosaminidase A deficiency in a young adult. Eur J Neurol. 2008;15(7):e70–1; author reply e2–3.
14. Holzer HT, Boschann F, Hennermann JB, Hahn G, Hermann A, von der Hagen M, et al. Cerebellar atrophy on top of motor neuron compromise as indicator of late-onset GM2 gangliosidosis. J Neurol. 2021.
15. Mascalchi M, Vella A (2018) Neuroimaging Applications in Chronic Ataxias. Int Rev Neurobiol 143:109–162
16. Oba H, Yagishita A, Terada H, Barkovich AJ, Kutomi K, Yamauchi T et al (2005) New and reliable MRI diagnosis for progressive supranuclear palsy. Neurology 64(12):2050–2055
17. Reetz K, Rodriguez-Labrada R, Dogan I, Mirzazade S, Romanzetti S, Schulz JB et al (2018) Brain atrophy measures in preclinical and manifest spinocerebellar ataxia type 2. Ann Clin Transl Neurol 5(2):128–137
18. Sugiyama A, Yokota H, Yamanaka Y, Mukai H, Yamamoto T, Hirano S et al (2020) Vertical pons hyperintensity and hot cross bun sign in cerebellar-type multiple system atrophy and spinocerebellar ataxia type 3. BMC Neurol 20(1):157
19. Klaes A, Reckziegel E, Franca MC Jr, Rezende TJ, Vedolin LM, Jardim LB et al (2016) MR Imaging in Spinocerebellar Ataxias: A Systematic Review. AJNR Am J Neuroradiol 37(8):1405–1412
20. Rattay TW, Lindig T, Baets J, Smets K, Deconinck T, Sohn AS et al (2019) FAHN/SPG35: a narrow phenotypic spectrum across disease classifications. Brain 142(6):1561–1572
21. Anheim M, Tranchant C, Koenig M (2012) The Autosomal Recessive Cerebellar Ataxias. N Engl J Med 366(7):636–646
22. Andronikou S, Pillay T, Gabuza L, Mahomed N, Naidoo J, Hlabangana LT et al (2015) Corpus callosum thickness in children: an MR pattern-recognition approach on the midsagittal image. Pediatr Radiol 45(2):258–272
23. Lefter S, O OM, Sweeney B, Ryan AM. Late-Onset Tay-Sachs Disease in an Irish Family. Mov Disord Clin Pract. 2021;8(1):106–10.
24. Godeiro-Junior C, Felicio AC, Benites V, Chieia MA, Oliveira AS (2009) Late-onset hexosaminidase A deficiency mimicking primary lateral sclerosis. Arq Neuropsiquiatr 67(1):105–106
25. Inzelberg R, Korczyn AD (1994) Parkinsonism in adult-onset GM2 gangliosidosis. Mov Disord 9(3):375–377
26. Patterson M. Niemann-Pick Disease Type C. In: Adam MP, Ardinger HH, Pagon RA, Wallace SE, Bean LJH, Mirzaa G, et al., editors. GeneReviews((R)). Seattle (WA)1993.
27. Steinlin M, Blaser S, Boltshauser E (1998) Cerebellar involvement in metabolic disorders: a pattern-recognition approach. Neuroradiology 40(6):347–354
28. Fagan N, Alexander A, Irani N, Saade C, Naffaa L (2017) Magnetic resonance imaging findings of central nervous system in lysosomal storage diseases: A pictorial review. J Med Imaging Radiat Oncol 61(3):344–352
29. Jadav RH, Sinha S, Yasha TC, Aravinda H, Gayathri N, Rao S et al (2014) Clinical, electrophysiological, imaging, and ultrastructural description in 68 patients with neuronal ceroid lipofuscinoses and its subtypes. Pediatr Neurol 50(1):85–95
30. D'Arco F, Hanagandi P, Ganau M, Krishnan P, Taranath A (2018) Neuroimaging Findings in Lysosomal Disorders: 2018 Update. Top Magn Reson Imaging 27(4):259–274
31. Chang YC, Huang CC, Chen CY, Zimmerman RA (2000) MRI in acute neuropathic Gaucher's disease. Neuroradiology 42(1):48–50
32. Majovska J, Nestrasil I, Paulson A, Nascene D, Jurickova K, Hlavata A et al (2021) White matter alteration and cerebellar atrophy are hallmarks of brain MRI in alpha-mannosidosis. Mol Genet Metab 132(3):189–197
33. MacQueen GM, Rosebush PI, Mazurek MF (1998) Neuropsychiatric aspects of the adult variant of Tay-Sachs disease. J Neuropsychiatry Clin Neurosci 10(1):10–19
34. Argov Z, Navon R (1984) Clinical and genetic variations in the syndrome of adult GM2 gangliosidosis resulting from hexosaminidase A deficiency. Ann Neurol 16(1):14–20

Molecular Genetics and Metabolism 132 (2021) 189–197

Contents lists available at ScienceDirect

Molecular Genetics and Metabolism

journal homepage: www.elsevier.com/locate/ymgme

White matter alteration and cerebellar atrophy are hallmarks of brain MRI in alpha-mannosidosis

Jitka Majovska [a,1], Igor Nestrasil [b,c,1], Amy Paulson [b], David Nascene [d], Katarina Jurickova [e], Anna Hlavata [e], Troy Lund [i], Paul J. Orchard [i], Manuela Vaneckova [f], Jiri Zeman [a], Martin Magner [a,g,*,2], Petr Dusek [f,h,**,2]

[a] Department of Pediatrics and Inherited Metabolic Disorders, First Faculty of Medicine, Charles University and General University Hospital, Prague, Czech Republic
[b] Division of Clinical Behavioral Neuroscience, Department of Pediatrics, University of Minnesota, Minneapolis, MN, USA
[c] Center for Magnetic Resonance Research, University of Minnesota, Minneapolis, MN, USA
[d] Department of Radiology, University of Minnesota, Minneapolis, MN, USA
[e] Center for Inherited Metabolic Disorders, Department of Paediatrics, National Institute of Children's Diseases and Faculty of Human Medicine, Comenius University in Bratislava, Bratislava, Slovakia
[f] Department of Radiology, First Faculty of Medicine, Charles University and General University Hospital, Prague, Czech Republic
[g] Department of Pediatrics, First Faculty of Medicine, Charles University and Thomayer Hospital, Prague, Czech Republic
[h] Department of Neurology and Center of Clinical Neuroscience, First Faculty of Medicine, Charles University and General University Hospital in Prague, Czech Republic
[i] Department of Pediatrics, Division of Blood and Marrow Transplantation, University of Minnesota, Minneapolis, MN, USA

ARTICLE INFO

Article history:
Received 1 October 2020
Received in revised form 24 November 2020
Accepted 24 November 2020
Available online 3 December 2020

ABSTRACT

Objective: Despite profound neurological symptomatology there are only few MRI studies focused on the brain abnormalities in alpha-mannosidosis (AM). Our aim was to characterize brain MRI findings in a large cohort of AM patients along with clinical manifestations.
Methods: Twenty-two brain MRIs acquired in 13 untreated AM patients (8 M/5F; median age 17 years) were independently assessed by three experienced readers and compared to 16 controls.
Results: Focal and/or diffuse hyperintense signals in the cerebral white matter were present in most (85%) patients. Cerebellar atrophy was common (62%), present from the age of 5 years. Progression was observed in two out of 6 patients with follow-up scans. Cortical atrophy (62%) and corpus callosum thinning (23%) were already present in a 13-month-old child. The presence of low T_2 signal intensity in basal ganglia and thalami was excluded by the normalized signal intensity profiling. The enlargement of perivascular spaces in white matter (38%), widening of perioptic CSF spaces (62%), and enlargement of cisterna magna (85%) were also observed. Diploic space thickening (100%), mucosal thickening (69%) and sinus hypoplasia (54%) were the most frequent non-CNS abnormalities.
Conclusion: White matter changes and cerebellar atrophy are proposed to be the characteristic brain MRI features of AM. The previously reported decreased T_2 signal intensity in basal ganglia and thalami was not detected in this quantitative study. Rather, this relative MR appearance seems to be related to the diffuse high T_2 signal in the adjacent white matter and not the gray matter iron deposition that has been hypothesized.

1. Introduction

Alpha-mannosidosis (AM; OMIM 248500) is a rare autosomal recessive lysosomal disorder caused by α-D-mannosidase enzyme deficiency due to pathogenic variants within the *MAN2B1* gene on chromosome 19p.13 [1,2]. The deficient enzyme activity leads to the lysosomal accumulation of undegraded oligosaccharides in the cells of multiple organ systems including the CNS. Brain disease mainly manifests by progressive intellectual disability, ataxia, hypotonia, epilepsy and psychiatric disorders including states of confusion, delusions, depression or anxiety. Overall, the disease is clinically variable with a continuum from severe forms with early death to milder forms with survival to adulthood [1]. Enzyme replacement therapy (ERT) and hematopoietic stem cell transplantation (HSCT) showed mixed or limited effects on the CNS [3,4].

There is limited information regarding brain MRI studies in this population, and prior reports have described a spectrum of abnormalities variably present in AM patients. Cerebral and cerebellar atrophy, vermis

* Correspondence to: M. Magner, Department of Pediatrics and Inherited Metabolic Disorders, First Faculty of Medicine, Charles University and General University Hospital, Ke Karlovu 2, 128 08 Praha 2, Czech Republic.
** Correspondence to: P. Dusek, Department of Neurology, First Faculty of Medicine, Charles University and General University Hospital, Katerinská 30, 128 08 Praha 2, Czech Republic.
E-mail addresses: martin.magner@vfn.cz (M. Magner), petr.dusek@vfn.cz (P. Dusek).
[1] These authors contributed equally to this work.
[2] Senior and corresponding authors.

https://doi.org/10.1016/j.ymgme.2020.11.008
1096-7192/

hypoplasia, widening of the diploë, skull disfiguration and enlarged perivascular spaces in the white matter have been reported [5–12]. High T_2 signal has been described in cerebral white matter, predominantly in the parieto-occipital region [6,7,10]. Additionally, decreased T_2 signal intensity in the basal ganglia suggestive of iron storage was described in two AM reports [5,9] with some authors suggesting a linkage to neurodegeneration with brain iron accumulation (NBIA) [9].

Here, we present the largest cohort described to date, including 13 patients that have not been previously analyzed or systematically studied. The aims of the present study were to estimate the prevalence, characterize the severity of abnormalities, and to propose potential neuroimaging outcome measures for future studies of alpha-mannosidosis.

2. Methods

2.1. Study participants

This retrospective study included patients with genetically and/or enzymatically confirmed diagnosis of AM and at least one brain MRI performed. Patients were followed in three clinical centers – First Faculty of Medicine at the Charles University, Prague, Czech Republic ($n = 5$); University of Minnesota ($n = 4$); and the National Institute of Children's Diseases, Comenius University in Bratislava, Slovakia ($n = 4$). 16 sex- and age-comparable control patients with no structural abnormalities on brain MRI were identified. Reasons for obtaining brain MRI were headache (in five individuals), fatigue, numbness, parasomnia, functional vertigo, tremor, staging of leukemia, epilepsy, perinatal asphyxia, failure to thrive, and retinoblastoma (each in one individual).

2.2. MRI parameters and assessments

A total of 22 MRI exams were available for 13 patients; seven patients had one MRI exam, four had two exams, one had three, and one had four MRI exams. Ten MRI exams were performed on 1.5 T and 12 MRI exams on 3 T MRI scanners, with ten patients having at least one scan at 3 T. Brain MRI abnormalities were assessed on routine clinical axial images acquired with following pulse sequences: T_2-weighted (T_2w) with echo time [TE]/repetition time [TR] = 80–112/3000–7250 ms, T_1-weighted (T_1w) with TE/TR = 2.2–15/8.3–596 ms), T_2-FLAIR (fluid attenuated inversion recovery) or T_2-TIRM (turbo inversion recovery magnitude) with TE/TR/inversion time [TI] = 65–385/2500–11,000/900–2500 ms. Susceptibility-weighted images (SWI) (TE/TR = 20/27 ms) were available in two and high-resolution magnetization-prepared rapid gradient-echo (MP-RAGE) (TE/TR/TI = 2.6–2.9/1900–2500/900–1100 ms) images were available in ten patients.

MRI datasets were available for 16 controls (5 females, median age at the time of MRI exam was 17 (range 1–30) years; five MRI exams were performed on 1.5 T and 12 MRI exams on 3 T clinical scanner. The assessment of MR signal intensity changes was always compared between an AM patient's scan and a corresponding age- and sex-matched control scan that were acquired at the same center and scanner using identical MRI pulse sequence parameters.

Three raters experienced in reading MRIs in rare disorders (IN, MV, PD) assessed all MRIs and systematically scored the presence and severity of predefined markers based on previous findings from AM case report studies: cerebellar, and cortical atrophy, corpus callosum thinning, enlargement of cisterna magna, enlargement of perivascular spaces, diffuse and focal/periventricular white matter signal abnormalities, T_2-hypointensities in deep gray matter nuclei (DGM), widening of perioptic CSF spaces, sinus hypoplasia and mucosal thickening, diploic space thickening, abnormalities of craniocervical junction, and appearance of sella Turcica; some of the abnormalities are shown in Fig. 1. White matter signal abnormalities were assessed as follows. Globally, the cerebral white/gray matter contrast was evaluated and further referred as diffuse high/hyperintense T_2 signal if the contrast was diminished. Focally, circumscribed periventricular T_2 hyperintensities were scored according to the extent (occipital/posterior horns, frontal/anterior horns, body of lateral ventricles, centrum semiovale, diffuse periventricular hyperintensity). Sinus hypoplasia was only assessed in patients seven years and older as sinuses are not completely formed prior to this age. All abnormalities were scored on the 3-point scale as (−) absent, (+) abnormal, and (++) very abnormal.

Diffuse high T_2 signal in white matter precluded reliable visual assessment of T_2-hypointensities in DGM. Therefore, a semiquantitative analysis was carried out to assess the white matter signal intensity of the supratentorial white matter and of the seemingly low T_2 signal in basal ganglia and thalami. First, the signal intensity of T_2w/T_2-FLAIR/T_2-TIRM images was normalized to CSF. This was achieved by dividing intensities of all single voxels by a mean ventricular CSF intensity. In the selected axial MR slice at the level of centrum semiovale, all CSF-normalized intensities from an oval region of interest encircling gray and white matter voxels were plotted in the signal intensity histogram (Fig. 2B and C). For DGM signal intensity profiling, in the selected axial MRI slice at the level of DGM (Fig. 2A and 3) a CSF-normalized signal intensity profile was generated from the row of voxels located within thalami and adjacent white matter (Fig. 3a). Histograms and profile plots of patients were compared to age-, sex-, and MRI- protocol matching controls (Figs. 2C, 3). The semiquantitative signal intensity analysis was performed in ImageJ (NIH, Bethesda, MD) [13].

2.3. Clinical findings

Medical history and physical examination were obtained. The following clinical data were evaluated: intellectual disability, ataxic gait, hearing and speech impairment, coarse facial features, short stature, heart disease, hepatomegaly, splenomegaly, adenoidectomy, tonsillectomy and frequent infections. Intellectual disability was scored on the 4-point scale as absent (−), mild (+), moderate (++), and severe or profound (+++) [14]. The other clinical signs were scored as absent (−), abnormal (+), and very abnormal (++). Short stature was defined as the height of patients below the 3rd population percentile.

2.4. Ethics

All information was accessed in accordance with the applicable laws and ethical requirements for the study period concerned and compliant with the Declaration of Helsinki, revised in 2000. All examined patients signed an informed consent for genetic testing. The study was approved by the Institutional Review Board (IRB) of the General University Hospital in Prague (Ethics Committee Approval Number: 1471/19). The data sharing was approved by the University of Minnesota IRB (code number: 1504E69081).

2.5. Data availability

De-identified individual participant data that underlie the results reported in this article will be shared upon reasonable request to one of the corresponding authors coming from researchers who provide a methodologically sound proposal.

3. Results

3.1. Patient characteristics

Demographics with clinical data of AM patients are summarized in Table 1. The median age at the onset of the first symptom was 9 months (range 0 months – 4 years) and the median diagnostic delay was 4.5 years (range 8 months – 35 years). The median age at the last clinical visit and at MRI exam was 17 years (range 13 months - 36 years). Intellectual disability was present in all patients spanning mild (three

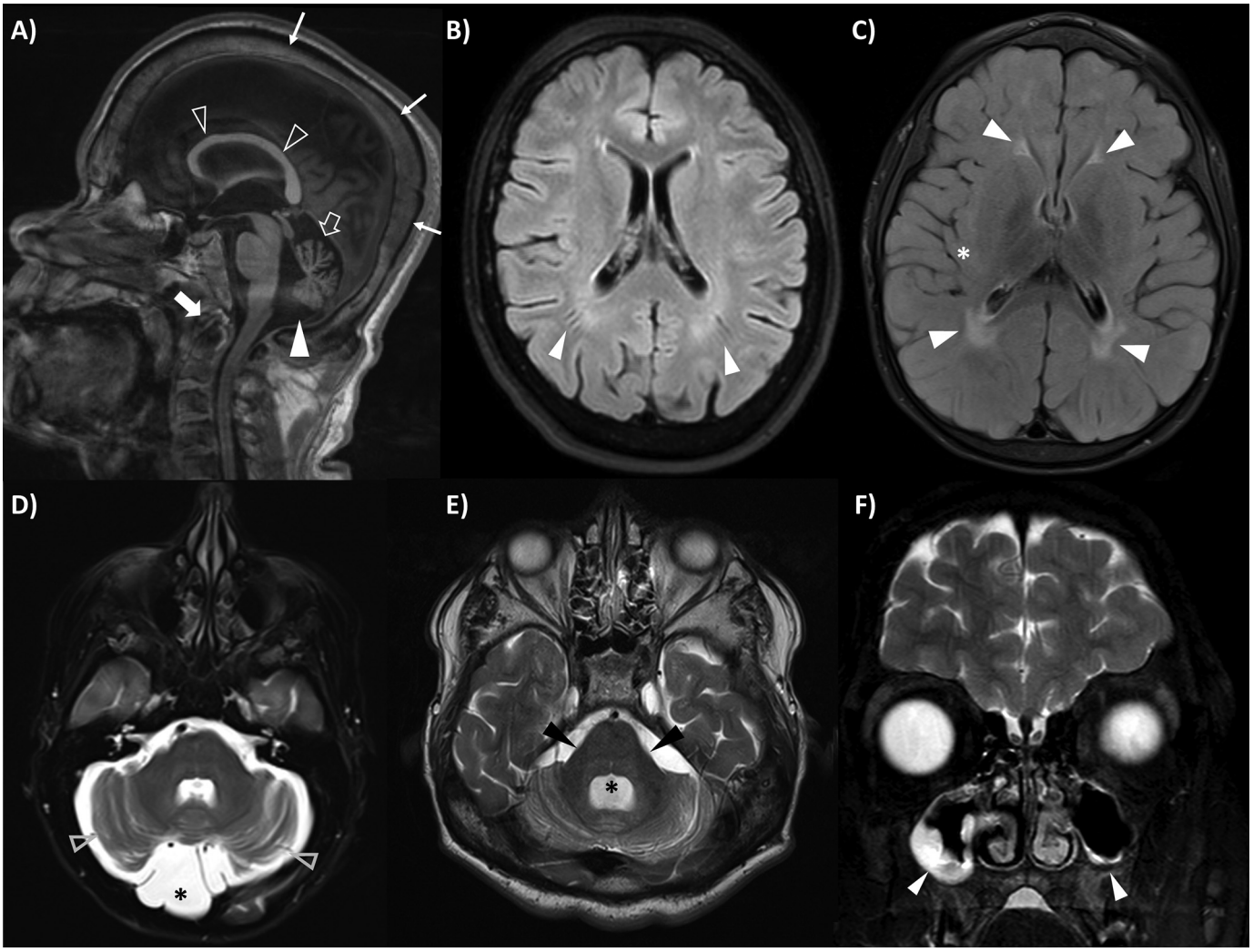

Fig. 1. A representative example of typical brain MRI abnormalities in alpha-mannosidosis. A) Thin corpus callosum (open arrowheads) and cerebellar vermis atrophy (open arrow), enlargement of cisterna magna (white arrowhead), abnormal craniocervical junction due to dens dysplasia (thick white arrow), and diploic space thickening (thin white arrows) on mid-sagittal T_1w image. B) Enlargement of perivascular spaces on T_2-FLAIR (white arrowheads) images. C) Diffuse increase of T_2 signal with focal T_2 hyperintensities in the periventricular white matter (white arrowheads) on axial T_2-FLAIR image in a 6-year-old patient; note low contrast between cerebral gray/white matter and seemingly hypointense deep gray matter (white asterisk). D) Cerebellar atrophy (empty arrowheads) and retrocerebellar cyst (asterisk) on axial T_2w image. E) Cerebellar atrophy with middle cerebellar peduncle thinning (black arrowheads) and enlargement of the 4th ventricle (black asterisk) on axial T_2w image. F) Mucosal thickening and hypoplasia of maxillary sinuses (white arrowheads) on coronal T_2w image; note also low cerebral gray/white matter contrast.

patients), moderate (five patients) and severe (five patients). Other neurological deficits included speech impairment (12/13; 92%) and ataxic gait (9/13; 69%). Hearing impairment and coarse facial features were constant findings across all patients. Heart disorder (5/9; 56%), short stature (6/13; 46%), hepatomegaly (6/13; 46%) and splenomegaly (4/13; 31%) were also present. Frequent infections were observed in eleven patients (11/13; 85%). Ten patients (10/13; 77%) underwent adenoidectomy and four patients (4/13; 31%) underwent tonsillectomy. No patients had been treated with HSCT or ERT at the time of MRI examination.

3.2. MRI findings

Brain MRI abnormalities in AM patients are summarized in Table 2 and representative example images shown in Fig. 1. Diffuse high T_2 signal in the white matter was rated abnormal or very abnormal in eleven patients (85%) resulting in a diminished contrast between gray and white matter on T_2w and/or T_2-FLAIR images (Fig. 2A and B). This finding was confirmed by visual histogram analysis showing narrower range of CSF-normalized signal intensities with a peak shifted to higher values in AM patients. Histogram difference of T_2 signals between patients and controls was greater at younger age and apparently diminished with increasing age (Fig. 2C).

Focal high T_2 signal intensities were seen in centrum semiovale or in the periventricular white matter areas around the occipital horns of the lateral ventricles (retrotrigonal areas) in 11 patients (85%) including two patients displaying a high T_2 signal around frontal horns of the lateral ventricles. No signal change in the cerebral white matter was observed only in two patients (15%).

On initial inspection, the basal ganglia and/or thalami were seemingly hypointense compared to the surrounding white matter in eight patients. However, this finding was difficult to attribute either to an isolated low T_2 signal within the DGM or to a higher contrast between DGM and white matter that exhibited an abnormally high signal in AM patients (Fig. 3). Based on the CSF-normalized signal intensity profiling, which quantitatively compared thalami and adjacent white matter at the level of basal ganglia, two findings were revealed. First, the signal of "seemingly" hypointense thalami did not differ between AM patients and

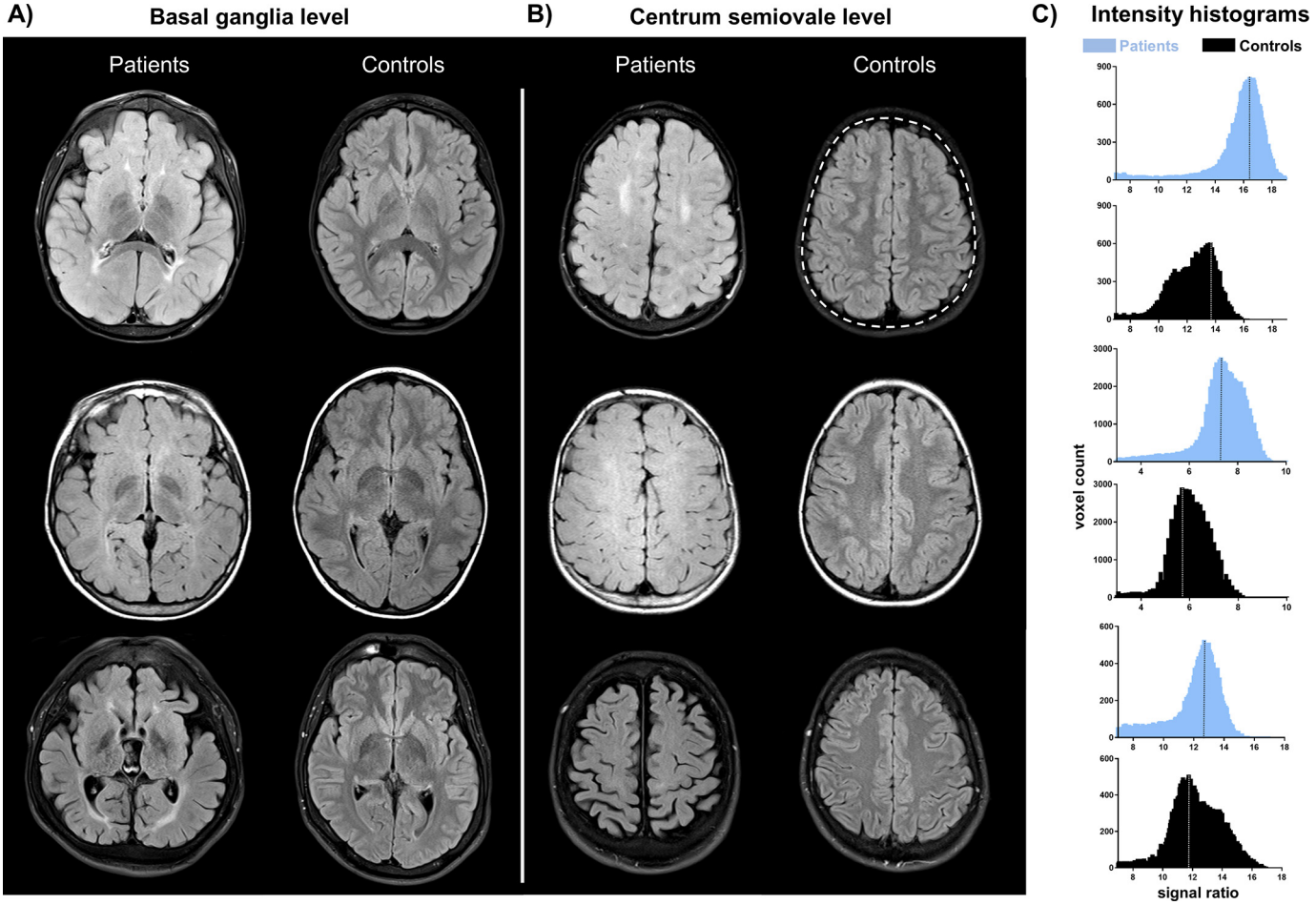

Fig. 2. Comparison of cerebral white/gray matter contrast and CSF-normalized signal intensity histograms in alpha-mannosidosis and control subjects. A) Images at the level of basal ganglia, and B) centrum semiovale with a CSF-normalized signal intensity from 3 T MR scanner; identical windowing was applied. C) Overall signal changes in patients with AM shown as intensity histograms of CSF-normalized signals in voxels calculated from an oval region of interest encircling brain tissue on single MR slices at the level of centrum semiovale (see dashed line circle as an example on the control image in the upper row in B). Please note that histograms presented in C (patient in blue color, controls in black color) correspond to the identical pair of patient/control images in the same row presented in B. Voxel distribution is shifted towards higher intensity values with a narrower range in AM patients compared to controls. Images of patient/control pairs in the upper/middle/bottom row were acquired at the age 6/8/27 years.

controls. Second, the white matter adjacent to thalami showed a higher signal intensity in AM patients that may consequently lead an MRI reading towards a false impression that thalami appear hypointense.

Cerebellar and diffuse cortical atrophy was revealed in eight patients (62%). Enlargement of cisterna magna was observed in 11 patients (85%). Neither cerebellar atrophy nor enlargement of cisterna magna were observed in the two youngest patients aged 1 and 3 years. Cerebellar atrophy progression was showed in two (33%) and cortical atrophy progression in three (50%) of six patients with available longitudinal scans. Only three patients (23%) had a corpus callosum thinning. The enlargement of perivascular spaces in white matter was observed in five (38%), and the widening of perioptic CSF spaces in eight (62%) patients.

Non-CNS abnormalities were diploic space thickening in all patients (100%) and sinus mucosal thickening in nine (69%). Paranasal sinus hypoplasia was found in seven out of nine patients (78%). Basilar impression and other craniocervical junction abnormalities were seen in three (23%) and J-shaped sella with enlarged suprasellar cistern were only present in one patient (8%) (Fig. 1). Progressive perioptic CSF spaces widening, perivascular spaces enlargement, diploic space thickening, and corpus callosum thinning were each present only once (17%) in six patients with MRI follow-up (Table 2).

In controls, MRI revealed hypoplastic frontal sinuses in three (27%) and sinus mucosal thickening in four (25%) individuals. Mucosal thickening affected mastoid, maxillary, and ethmoid with maxillary sinuses, each represented once in the entire control cohort. Diploic space thickening was seen in one (6%) and the enlargement of cisterna magna together with J-shaped sella were observed in one (6%) control subject.

4. Discussion

AM is an ultra-rare progressive disease [2] and reports of brain MRI findings in AM patients are very sparse [5–10]. The current MRI study is the largest to date, characterizing the prevalence and the severity of main pathological features in 13 patients with alpha-mannosidosis across three centers. Focal and diffuse cerebral white matter abnormalities with cerebellar and cortical atrophy were the most frequent CNS findings. In some patients with follow up MRI, progressive atrophy of the cerebrum (33%) and cerebellum (50%) was noted. Basal ganglia and/or thalami were seemingly hypointense compared to the surrounding white matter. However, the normalized signal intensity profiling did show that the thalamic MRI intensity signal was comparable between AM and control subjects, and higher in the adjacent white matter in AM patients than controls.

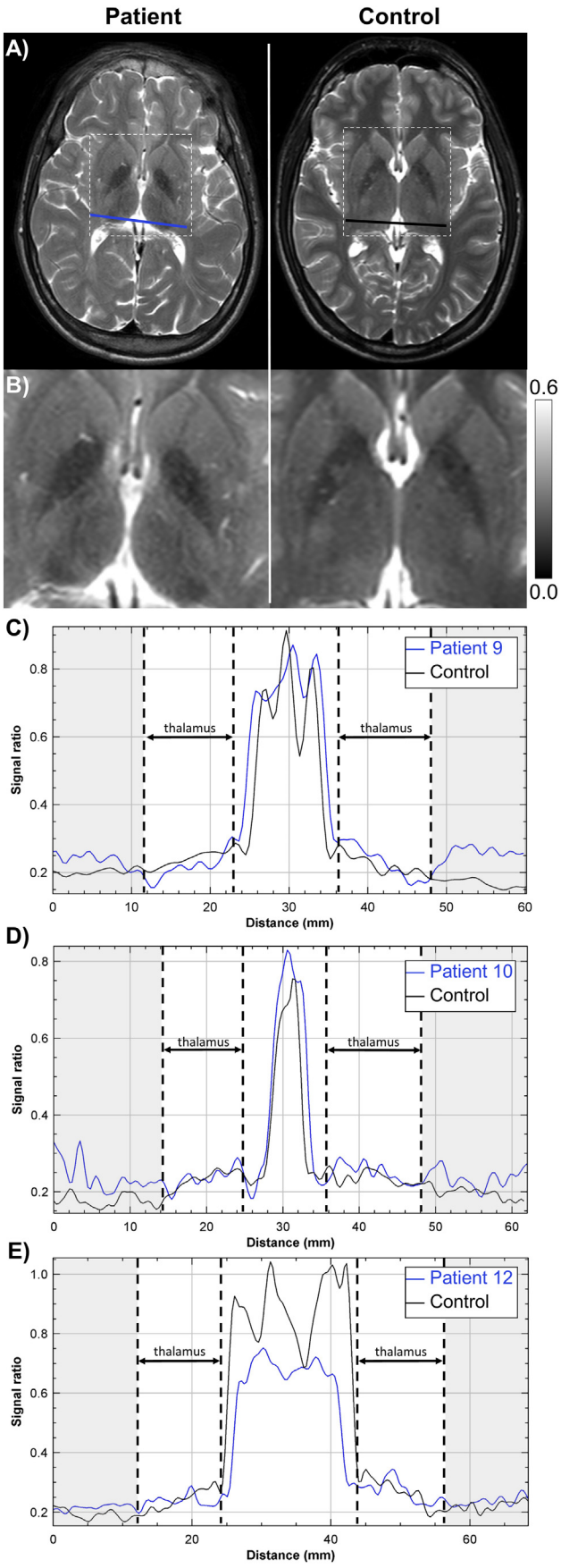

Abnormally high white matter signal was almost universal finding in our cohort that corroborates with previous MRI and histopathological studies in animal models [15–19] and AM patients [6–8,10,20]. Additionally, focal T_2 hyperintensities were described in the white matter of the centrum semiovale and/or of the periventricular area mostly pronounced in retrotrigonal region [6–8]. In general, such changes may suggest age-inappropriate myelination, gliosis, cellular swelling, or shifts in water content [6,10]. Higher T_2 signal intensity in the white matter indicating more severe abnormality in younger compared to older AM patients suggests hypomyelination as a potential etiology. This is further supported by the localization of focal T_2 hyperintensities in the periventricular white matter, which are the predilection zones of the delayed myelination [21–23]. These terminal zones are located around the frontal and occipital horns of the lateral ventricles. One of the last regions to mature in T_2w image, typically at the age three years, is the peritrigonal/retrotrigonal zone that is located around/behind the trigone of the lateral ventricle [21,23], often called "terminal zones". The presence of high T_2 signal in retrotrigonal area was reported in case report studies [6–8,10] and detected in almost all AM subjects in our cohort. The finding is typical for an hypomyelination and in our AM patients, it was detected past three years of age even in adolescence and adulthood.

Underlying white matter histopathology was examined in feline and guinea pig AM models [15,17,19] and in case reports of deceased AM patients [20,24]. Neuronal lysosomal vacuolation, widespread axonal and dendritic spheroids, myelin loss, glial swelling, reactive gliosis, and neuronal numeric atrophy in the cerebrum, brainstem, and cerebellum were observed in AM cats and guinea pigs [15,17,19]. Similarly, neuronal cytoplasmic vacuolation and diffuse neuronal and myelin loss with white matter gliosis in cerebrum, and Purkinje cell spheroids, loss of Purkinje and internal granule cells in cerebellum were reported at autopsy in deceased AM patients [20,24].

In AM cats, the histopathological findings correlated with neuroimaging. Gray and white matter impairment at the microstructural level (myelin, axons, water content) with the presence of gliosis were assessed by magnetization transfer [19], T_2 mapping [17] and diffusion weighted imaging parameters [16–18]. The histological evidence of

Fig. 3. Normalized signal intensity profiling of deep gray matter nuclei. A) Axial T_2 images with CSF-normalized signal intensity in AM patient (left) and control (right) in the level of basal ganglia; identical image windowing was applied. Blue (patient) and black (control) lines represent the selected row of voxels for the profiling. Images outlined by dashed squares were extracted, zoomed in and shown in B. B) Detailed view of the basal ganglia and thalamus region. Basal ganglia display comparable signal intensity in globus pallidus while thalamus is relatively hypointense in the AM patient (left). The scale denotes signal intensity ratio (i.e. voxel intensity divided by mean intensity of ventricular CSF). C) Signal profile plot of patient 9 at the age 17 years and age-matched control (corresponding T_2 images shown in A). D) Signal profile plot in patient 10 at the age 28 years and age-matched control. E) Signal profile plot in patient 12 at the age 27 years and age-matched control. All signal profile plots derived from T_2 images acquired at 3 T field strength are shown for similar locations in all patients as indicated by example lines in A. On x-axis, the distance was measured from the anatomical right (0 mm) to the anatomical left (60 mm) on lines showed as the example in A. The lines were centered at 30 mm, which corresponds to the midsagittal plane. The peak around the distance of 30 mm corresponds to high-intensity CSF voxels originating from the third ventricle. Thalamic parts of the plot are demarcated by dashed lines while gray-colored columns mark white matter laterally adjacent to thalami in C-E. On y-axis, intensity signal ratios are shown. The signal profile plots corresponding to thalamic normalized signals are comparable in each patient/control pair. Normalized signals in adjacent white matter are distinctly increased in patient 9 (C). The finding corroborates with diffuse white matter T2 signal increase that was visually rated as very abnormal (see Table 2). Less remarkable and virtually no increase of white matter signals is observed in patient 10 (D) and 12 (E), respectively; diffuse increase of white matter T_2 signal was visually rated as abnormal in both of these patients. Please note that lower CSF signal ratio in patient 12 (E) is a flow void effect caused by faster CSF flow in the caudal part of the third ventricle.(For interpretation of the references to color in this figure legend, the reader is referred to the web version of this article.)

Table 1
Clinical data of 13 patients with alpha-mannosidosis.

	Patient 1	Patient 2	Patient 3	Patient 4	Patient 5	Patient 6	Patient 7	Patient 8	Patient 9	Patient 10	Patient 11	Patient 12	Patient 13
Sex	M	F	F	M	F	M	M	M	M	M	F	M	F
Age at first symptom	9 months	4 months	6 months	2 years	3 months	0 month	3 years	4 years	9 months	12 months	3 years	6 months	1 month
Age at diagnosis	17 months	4 years	2 years	4 years	7 years	9 years	5 years	13 years	15 years	3 years	22 years	5 years	36 years
Current age (age at the last MRI)	13 months	4 years	5 years	6 years	8 years	9 years	18 years	17 years	17 years	28 years	32 years	27 years	36 years
Intellectual Disability	++	+	+++	++	+	++	+	++	++	+++	+++	+++	+++
Ataxic gait	−	+	++	−	−	−	+	+	+	++	++	++	++
Hearing impairment	++	+	+	++	++	++	+	++	++	++	++	++	++
Speech impairment	+	+	++	−	+	+	+	+	+	+	++	++	+
Coarse facial features	+cranio-synostosis	+cranio-synostosis	+	+	++	+	+cranio-synostosis	++	++	++	++	++	++
Short stature	−	−	−	−	−	+	+	+	+	−	+	+	−
Heart disease	−	n/a	−	viral myocarditis, heart transplant at age 4 months	n/a	−	history of pericardial effusion	pulmonary insufficiency Ist degree	n/a	Hyper-echogenic aortic valve	−	aortal insufficiency Ist degree	n/a
Hepatomegaly	+	−	−	−	−	−	++	+	−	+	−	+	+
Splenomegaly	+	−	−	−	++	−	−	+	−	−	−	−	+
Adenoidectomy	−	−	+	+	+	+	+	+	+	+	+	+	−
Tonsillectomy	−	−	−	−	−	+	+	−	−	−	+	+	−
Frequent infections	+	+	−	−	+	+	+	+	+	+	+	+	+
Diagnosis confirmation by genotyping or enzyme activity	low enzyme* activity†, genetic analysis in progress	c.2248C > T/ c.2248C > T	low enzyme* activity†, genetic analysis not done	p.Y401X/full gene deletion	c.979_980delAT/ c.979_980delAT	c.2248C > T/ c.2248C > T	low enzyme* activity†, genetic analysis not done	c.856G > A/ c.856G > A	c.979_980delAT/ c.979_980delAT	c.2248C > T/ c.2248C > T	low enzyme* activity†, genetic analysis not done	c.2248C > T/ c.2248C > T	c.979_980delAT/ c.2248C > T

M male, **F** female; *α-D-mannosidase; †below 5% of enzyme activity; **n/a** not available.
Intellectual disability was scored on the 4-point scale as absent (−), mild (+), moderate (++), and severe or profound (+++). Short stature was defined as the height of patients below the 3rd population percentile. The other clinical signs were scored as absent (−), abnormal (+), and very abnormal (++).

Table 2
Neuroimaging characteristics in alpha-mannosidosis patients.

	Patient 1	Patient 2	Patient 3	Patient 4	Patient 5	Patient 6	Patient 7	Patient 8	Patient 9	Patient 10	Patient 11	Patient 12	Patient 13
Sex	M	F	F	M	F	M	M	M	M	M	F	M	F
Age at MRI	13 months	4 years	5 years	5/6 years	8 years	9 years	9/10/16/18 years	13/17 years	13/17 years	22/24/28 years	23/32 years	27 years	36 years
MRI field strength (T)	1.5	3	1.5	1.5/3	3	3	1.5/1.5/3/3	3/3	1.5/3	1.5/1.5/3	1.5/1.5	3	3
Diffuse increase of T2-signal in WM	+	+	++	++	++	+	−	+	++	+	−	+	+
Focal T2 hyperintensities in periventricular WM	+	+	+	++	+	+	−	++	+	+	−	+	+
Enlargement of cisterna magna	—	−	+	+	+	+	+	++	++	+	++	++	+
Cerebellar atrophy	−	−	+	−/+	−	−	−	+	+	+/+/++	+	+	++
Cortical atrophy	+	−	+	−/+	−	−	−/−/+/+	+	−	−/−/+	+	++	−
Corpus callosum thinning	+	−	−	−/+	−	−	−	−	−	−	−	+	−
Enlargement of perivascular spaces in WM	−	+	−	−	−	+	−/−/+/+	−	+	−	−	−	+
Widening of perioptic CSF spaces	+	+	+	+	++	−	+	−/+	++	−	−	−	−
Sinus hypoplasia *location*	n/a	n/a	n/a	n/a	−	+maxillary, frontal, sphenoid	+frontal, mastoid	+ +maxillary, sphenoid	+maxillary, frontal, sphenoid, mastoid	+mastoid	−	+maxillary	+mastoid
Mucosal thickening *location*	−	+sphenoid	−	+ethmoid	+maxillary, ethmoid	−	+sphenoid	+ethmoid	+maxillary, ethmoid	+maxillary, ethmoid	−	+maxillary, ethmoid	+ethmoid
Basilar impression/craniocervical junction abnormalities	−	−	−	−	−	−	−	+	+	−	−	+	−
Diploic space thickening	+	+	+	+	++	+	++	+/++	+	+	+	++	++
Sella Turcica abnormalities	−	−	−	−	−	−	+ J-shaped sella, enlarged suprasellar cistern	−	−	−	−	−	−

Age at MRI is shown for each longitudinal scan. Ratings of each longitudinal scan are shown if an abnormality changed overtime.
M male, **F** female; **WM** white matter, **CSF** cerebrospinal fluid, **T** Tesla, **n/a** not available, assessment not possible because sinuses are not developed at this age yet.

abnormal myelin, neuronal and glial swelling, and gliosis was linked to MRI signal abnormalities measured in the cerebrum and cerebellum. The most recent study of gene therapy in feline AM model proposed that the therapeutic response could be measured by diffusion weighted imaging parameters [18].

In attempts to elucidate the presence and the etiology of white matter changes, MR spectroscopy (MRS) studies measured spectra from single voxel (volume-of-interest) using short echo time (TE) [7,10]. Metabolite ratios of myo-inositol/creatine, which is a potential glial cells marker, and choline/creatine, which is a marker of accelerated cell-membrane turnover (e.g. in active de−/remyelination, inflammation or gliosis [25]) were quantified. MR spectra were acquired from parieto-occipital white matter and/or centrum semiovale [7,10]. Increased choline/creatine and myo-inositol/creatine ratios when compared to controls were only detected in the parieto-occipital white matter [10]. This result may relate to reduced myelination, age-inappropriate myelination in this region or potentially to gliosis or inflammation. In contrast, higher myo-inositol/creatine ratio in AM patients and comparable choline/creatine ratio to controls were found in the centrum semiovale [7], which is in support of gliotic changes in this brain region.

AM and other lysosomal disorders of oligosaccharide storage such as fucosidosis, GM1 gangliosidosis, and mucolipidosis type IV were previously suggested as the NBIA spectrum diseases in narrative reviews [26,27]. Decreased T_2 signal in thalami was proposed as a sign of lysosomal storage disease [28] and as a sign suggestive of iron accumulation in basal ganglia and thalami, reported in two AM patients [5,9]. The findings of diffuse hyperintense white matter compared to relative hypointense basal ganglia and thalami was observed also in our patients. However, we found that the normalized signal intensity profiling demonstrated that the signal of "seemingly" hypointense thalami was not different between AM patients and controls. The degree of basal ganglia T_2 hypointensity typically seen in core NBIA syndromes was not present in any AM subject. The finding was further supported by a higher signal in white matter adjacent to thalami of AM patients, which may explain why thalami or basal ganglia seemed more hypointense in AM than in controls. Our findings suggest that apparent T_2 hypointensity in deep gray matter is a consequence of abnormal surrounding white matter rather than DGM pathology. We oppose the iron accumulation hypothesis and the inclusion of AM in the NBIA disease group.

We found cortical and cerebellar atrophy in more than half of the patients, which is comparable to the previously reported prevalence [5–7,10]. Although the lower frequency of cortical atrophy was ascribed to the younger age in the previously reported AM cohort (range 7–17 years; mean age 12.3 years) [10], we showed cortical atrophy in very early age as documented in our youngest 13-month-old patient. This suggests that supratentorial degenerative changes may begin in early childhood and progress through adulthood in most AM cases.

Cerebellar atrophy was reported in patients who were either in their late teens [5] or older [6,7]. In our study, cerebellar atrophy was observed in a 5-year-old patient but not in the 13-month or 3-year-old patient. Additionally, cerebellar atrophy became more frequent with increasing age. In two out of six patients with longitudinal scans a clear progression of cerebellar atrophy was observed. The findings are in agreement with pathological description of the atrophic cerebellum, especially the vermis, in a 4.5-year-old boy [20]. Cisterna magna enlargement invariably accompanied cerebellar atrophy in our cohort, but was also observed in two patients aged 8 and 9 years without cerebellar atrophy. Animal models of lysosomal storage disorders confirmed relatively normal initial development of cerebellum followed by degenerative changes and progressive atrophy beginning very early in life and initially affecting the vermis [29,30]. As such, it is possible that enlargement of the cisterna magna in AM in humans may be a consequence of preferential volume loss in the cerebellar vermis. In AM guinea pig model, the histopathologic changes such as neuronal lysosomal vacuolation, axonal spheroids and reduced white matter myelination were shown from birth preceding the onset of neurologic abnormalities. Subsequently, these changes rapidly progressed and were accompanied with other abnormalities including loss of cerebellar Purkinje cells [15] that may then eventually manifest as cerebellar atrophy. Notably, cerebellar atrophy was associated with ataxia and none of our patients with very abnormal neuroimaging abnormalities in the posterior fossa was ataxia-free. Moreover, mild ataxic gait occurred before the development of discernible cerebellar atrophy in two patients. The enlargement of perivascular spaces in the white matter was found in 38% of our patients, which corresponds to the previous studies [8,10]. The widening of perioptic CSF spaces was found in 62% of our patients and in one of three patients in the study by Patlas et al. [8]. Prominent CSF space around the optic nerves can be a marker of increased intracranial pressure. Other MRI signs of intracranial hypertension were not observed except for one patient with empty sella Turcica. No clinical signs of intracranial hypertension were observed in our cohort.

Other non-CNS abnormalities were recognized on the brain MRI such as sinus hypoplasia, mucosal thickening, diploic space thickening or basilar impression and their prevalence was comparable with previous studies [5–8]. Patlas et al. described two AM patients with tight foramen magnum with descent of tonsils and a syrinx in the cervical spinal cord in one of the patients. These abnormalities were not found in our cohort. J-shaped sella Turcica, a finding previously described in several lysosomal storage disorders [31–33] was previously reported in one patient [8]. Other studies described AM cases of an enlarged suprasellar cistern associated with an elongated hypothalamic infundibulum [8] or partial empty sella [6]. In our control cohort, J-shaped sella was also present in one control subject indicating that sella Turcica abnormalities are rather incidental than associated with AM[33].

The main limitation of our study was its retrospective nature, which did not allow MR scanning protocol harmonization. MR images from different centers were acquired on different scanners with 1.5 and 3 T magnetic field strengths and different pulse sequence parameters. This fact hampers inter-center comparability as well as assessment of longitudinal changes. It also precludes quantitative analyses. Objectivity of the assessment in our study was improved by comparison of pairs of patient's MR scan to corresponding control's scan, both acquired at the same center on the identical scanner using the identical MR pulse sequence parameters.

5. Conclusion

Abnormal cerebral white matter T_2 hyperintense signal suggestive of white matter cerebral disease or abnormal myelination and atrophy of the cerebrum and cerebellum starting in early childhood were predominant in this AM cohort. The MRI findings were accompanied by intellectual disability in all patients and speech impairment and ataxic gait in most patients. We suggest assessing white matter integrity and cerebral and cerebellar atrophy by quantitative MRI approaches in future studies and clinical trials.

The "hypointense" appearance of basal ganglia and thalami in T_2w was explained by a higher signal in the white matter and the previously suggested iron accumulation in brain MRI of AM patients was not confirmed in this study. One must interpret MRI in AM with great caution to avoid perpetuating misconception and future quantitative studies using iron-susceptible imaging techniques are warranted to elucidate the iron accumulation controversy.

Acknowledgements

The work was supported by the grants from the Ministry of the Health of the Czech Republic RVO-VFN-64165/2012 and the Ministry of Education, Youth and Sport of the Czech Republic PROGRES Q32/LF2.

IN was funded by the Lysosomal Disease Network (U54NS065768) that is a part of the Rare Diseases Clinical Research Network (RDCRN),

an initiative of the Office of Rare Diseases Research (ORDR), and NCATS. This consortium is funded through a collaboration between NCATS, NINDS, and NIDDK.

References

[1] D. Malm, O. Nilssen, Alpha-mannosidosis, Orphanet J. Rare Dis. 3 (2008) 21.
[2] N. Guffon, A. Tylki-Szymanska, L. Borgwardt, et al., Recognition of alpha-mannosidosis in paediatric and adult patients: presentation of a diagnostic algorithm from an international working group, Mol. Genet. Metab. 126 (2019) 470–474.
[3] M.R. Ceccarini, M. Codini, C. Conte, et al., Alpha-Mannosidosis: therapeutic strategies, Int. J. Mol. Sci. 19 (2018).
[4] L. Borgwardt, N. Guffon, Y. Amraoui, et al., Efficacy and safety of Velmanase alfa in the treatment of patients with alpha-mannosidosis: results from the core and extension phase analysis of a phase III multicentre, double-blind, randomised, placebo-controlled trial, J. Inherit. Metab. Dis. 41 (2018) 1215–1223.
[5] J.R. Ara, E. Mayayo, M.E. Marzo, et al., Neurological impairment in alpha-mannosidosis: a longitudinal clinical and MRI study of a brother and sister, Childs Nerv. Syst. 15 (1999) 369–371.
[6] J.L. Dietemann, M.M. Filippi de la Palavesa, C. Tranchant, B. Kastler, MR findings in mannosidosis, Neuroradiology 32 (1990) 485–487.
[7] A. Gutschalk, I. Harting, M. Cantz, C. Springer, K. Rohrschneider, H.M. Meinck, Adult alpha-mannosidosis: clinical progression in the absence of demyelination, Neurology 63 (2004) 1744–1746.
[8] M. Patlas, M.Y. Shapira, A. Nagler, R. Sheffer, J.M. Gomori, MRI of mannosidosis, Neuroradiology 43 (2001) 941–943.
[9] E. Zoons, T.J. de Koning, N.G. Abeling, M.A. Tijssen, Neurodegeneration with brain iron accumulation on MRI: an adult case of alpha-mannosidosis, JIMD Rep. 4 (2012) 99–102.
[10] L. Borgwardt, E.R. Danielsen, C. Thomsen, et al., Alpha-mannosidosis: characterization of CNS pathology and correlation between CNS pathology and cognitive function, Clin. Genet. 89 (2016) 489–494.
[11] S. Niemann, M. Beck, G. Seidel, J. Spranger, P. Vieregge, Neurology of adult alpha-mannosidosis, J. Neurol. Neurosurg. Psychiatry 61 (1996) 116–117.
[12] R. Govender, L. Mubaiwa, Alpha-mannosidosis: a report of 2 siblings and review of the literature, J. Child Neurol. 29 (2014) 131–134.
[13] C.A. Schneider, W.S. Rasband, K.W. Eliceiri, NIH image to ImageJ: 25 years of image analysis, Nat. Methods 9 (2012) 671–675.
[14] American Psychiatric Association (APA), Diagnostic and Statistical Manual of Mental Disorders, 5th ed. APA, Washington, DC, 2013.
[15] A.C. Crawley, S.U. Walkley, Developmental analysis of CNS pathology in the lysosomal storage disease alpha-mannosidosis, J. Neuropathol. Exp. Neurol. 66 (2007) 687–697.
[16] M. Kumar, J.T. Duda, S.Y. Yoon, et al., Diffusion tensor imaging for assessing brain gray and white matter abnormalities in a feline model of alpha-mannosidosis, J. Neuropathol. Exp. Neurol. 75 (2016) 35–43.
[17] C.H. Vite, S. Magnitsky, D. Aleman, et al., Apparent diffusion coefficient reveals gray and white matter disease, and T2 mapping detects white matter disease in the brain in feline alpha-mannosidosis, AJNR Am. J. Neuroradiol. 29 (2008) 308–313.
[18] S.Y. Yoon, J.E. Hunter, S. Chawla, et al., Global CNS correction in a large brain model of human alpha-mannosidosis by intravascular gene therapy, Brain 143 (2020) 2058–2072.
[19] C.H. Vite, J.C. McGowan, K.G. Braund, et al., Histopathology, electrodiagnostic testing, and magnetic resonance imaging show significant peripheral and central nervous system myelin abnormalities in the cat model of alpha-mannosidosis, J. Neuropathol. Exp. Neurol. 60 (2001) 817–828.
[20] B. Kjellman, I. Gamstorp, A. Brun, P.A. Ockerman, B. Palmgren, Mannosidosis: a clinical and histopathologic study, J. Pediatr. 75 (1969) 366–373.
[21] H.M. Branson, Normal myelination: a practical pictorial review, Neuroimaging Clin. N. Am. 23 (2013) 183–195.
[22] S.M. Maricich, P. Azizi, J.Y. Jones, et al., Myelination as assessed by conventional MR imaging is normal in young children with idiopathic developmental delay, AJNR Am. J. Neuroradiol. 28 (2007) 1602–1605.
[23] C. Parazzini, C. Baldoli, G. Scotti, F. Triulzi, Terminal zones of myelination: MR evaluation of children aged 20-40 months, AJNR Am. J. Neuroradiol. 23 (2002) 1669–1673.
[24] J.H. Sung, M. Hayano, R.J. Desnick, Mannosidosis: pathology of the nervous system, J. Neuropathol. Exp. Neurol. 36 (1977) 807–820.
[25] K.T. Fernando, M.A. McLean, D.T. Chard, et al., Elevated white matter myo-inositol in clinically isolated syndromes suggestive of multiple sclerosis, Brain 127 (2004) 1361–1369.
[26] P. Dusek, S.A. Schneider, Neurodegeneration with brain iron accumulation, Curr. Opin. Neurol. 25 (2012) 499–506.
[27] P. Dusek, J. Jankovic, W. Le, Iron dysregulation in movement disorders, Neurobiol. Dis. 46 (2012) 1–18.
[28] T. Autti, R. Joensuu, L. Aberg, Decreased T2 signal in the thalami may be a sign of lysosomal storage disease, Neuroradiology 49 (2007) 571–578.
[29] S.L. Macauley, R.L. Sidman, E.H. Schuchman, T. Taksir, G.R. Stewart, Neuropathology of the acid sphingomyelinase knockout mouse model of Niemann-pick a disease including structure-function studies associated with cerebellar Purkinje cell degeneration, Exp. Neurol. 214 (2008) 181–192.
[30] J. Sikora, S. Dworski, E.E. Jones, et al., Acid Ceramidase deficiency in mice results in a broad range of central nervous system abnormalities, Am. J. Pathol. 187 (2017) 864–883.
[31] D.I. Zafeiriou, S.P. Batzios, Brain and spinal MR imaging findings in mucopolysaccharidoses: a review, AJNR Am. J. Neuroradiol. 34 (2013) 5–13.
[32] L. Giugliani, C.E. Steiner, C.A. Kim, et al., Clinical findings in Brazilian patients with adult GM1 gangliosidosis, JIMD Rep. 49 (2019) 96–106.
[33] M. Yang, S.Y. Cho, H.D. Park, et al., Clinical, biochemical and molecular characterization of Korean patients with mucolipidosis II/III and successful prenatal diagnosis, Orphanet J. Rare Dis. 12 (2017) 11.